



NASA Human Exploration Rover

May 5, 2021

Team: Hannah Kijowski, Kilian Moran,

Brooke Grossmann, Evan Rubio, Aaron Lee, Jaime Rodriguez Cervantes

Abstract

The Galileo Rover is a continuation of previous rover teams at the University of Colorado Denver. Each year NASA hosts its Human Exploration Rover Challenge in Huntsville, Alabama. This challenge allows high school and International collegiate teams the opportunity to put their rover designs to the test on a NASA designed obstacle course. The Galileo Rover team is collectively seeking first place in competition this April 2021 and our main objective is to win the overall competition award. This award is going to challenge us to be the best in the following categories; design reviews, safety, educational engagement, and most importantly a successful excursion. The Galileo Rover team will keep the current wheel design from last year's rover team, allowing for the reduction of weight in each wheel and strengthening its integrity while completing the obstacle course. The team has plans to finish manufacturing and assembly of the wheel. In order to meet size constraints and to fit in a 5'x5'x5' cube as well as weighing less than 210lbs, as specified by the competition, the team will keep the Endeavour's hinge design allowing the front pedal to fold inward. In order to reduce torsion in the frame as previous teams have had causing the steering to malfunction, the Galileo frame will either adopt last year's torsion plate design or use epoxies to connect the hardware to the carbon fiber tubes. The Galileo team will be continuing to analyze the latest steering design that Endeavor finalized on. This will consist of two pitman arms connected to a bulkhead and two rods which will form a parallelogram. The steering will remain a linear steering design, and adjustments will be made to the suspension in order to provide more stability and less chance of failure during competition.

Table of Contents

ABSTRACT	2
LIST OF FIGURES	4
INTRODUCTION	6
RIDER SELECTION	9
<i>INTRODUCTION</i>	9
<i>WELLNESS CENTER TESTING</i>	9
<i>POWER TO WEIGHT RATIOS</i>	10
<i>INCLINE CLIMBING VELOCITY</i>	10
<i>RESULTS</i>	12
GALILEO FRAME	12
<i>DESIGN</i>	12
<i>SEATS</i>	19
GALILEO DRIVETRAIN	26
<i>GEAR RATIOS</i>	26
<i>GEAR SELECTOR</i>	30
GALILEO STEERING	31
<i>STEERING DESIGN</i>	31
<i>CALIPER MOUNT</i>	33
<i>UPPER A-ARM</i>	36
<i>TIE ROD CONNECTION</i>	37
<i>STEERING BRACKET</i>	39
<i>PATH FORWARD</i>	41
<i>HANDLE DESIGN</i>	41
<i>TASKS</i>	44
GALILEO WHEELS	48
<i>DESIGN</i>	48
<i>HUB ASSEMBLY</i>	50
<i>TESTING</i>	53
<i>MANUFACTURING</i>	54
<i>MANUFACTURING OF SPOKES</i>	58
<i>WHEEL ASSEMBLY</i>	60
<i>WHEEL FOAM POUR</i>	63
<i>AREAS FOR IMPROVEMENT</i>	66
BUDGET/COSTS	68
GANTT DIAGRAMS	69
REFERENCES	70
APPENDICES	71
<i>APPENDIX A: ESTIMATED BUDGET</i>	71
<i>APPENDIX B: UPDATED BUDGET</i>	72
<i>APPENDIX C: BREAKING AT HUB</i>	73
<i>APPENDIX D: HOOP STRESS</i>	74
<i>APPENDIX E: SIDEWALL THICKNESS</i>	75
<i>APPENDIX F: BENDING AT HUB</i>	76
<i>APPENDIX G: FLEX FOAM DATA SHEET</i>	77
<i>APPENDIX H: EQUATIONS FOR GEAR RATIO CALCULATIONS</i>	78

List of Figures

Figure 1: Free body diagram showing rover acceleration on an incline	11
Figure 2: MDF Torsion Plate Mold	14
Figure 3: Torsion Plate Mold from Fusion 360	14
Figure 4: MDF Torsion Plate Tool and Carbon Fiber Plates	16
Figure 5: "S" Torsion Plate and Manufactured Carbon Fiber Torsion Plate	16
Figure 6: Breather Cloth & Peel Ply, Vacuum Bagging of Carbon Fiber Layup	17
Figure 7: Frame and Suspension Assembly(left), Torsion Plates under Seats(right)	18
Figure 8: Seats Attached to the Frame(left), Seat Foam & 4-point Seat Belts(right)	19
Figure 9: Front Suspension Assembly	21
Figure 10: Rear Suspension Assembly(left), Two-gear Belt System (right)	21
Figure 11: New Hollow Rod(left) and Solid Rod(right).....	22
Figure 12: Rear Suspension Pivot Components on Fusion 360.....	24
Figure 13: Stringer Inserts with brass fitting(left), Drive train gear with brass fitting(right).....	24
Figure 14: Photo of Suspension with Torsion Plates Attached to Frame	25
Figure 15: Free Body Diagram of Rover on Incline	27
Figure 16: Free Body Diagram of a Wheel on the Rover	28
Figure 17: Relationship Between Input Gear and Output Gear	28
Figure 18: Relationship between the Surface Angle and Velocity	29
Figure 19: Top down view of steering design assembly with handles	32
Figure 20: Back view of steering assembly	32
Figure 21: Close up of Tie Rod Connection Top Pitman Arm to Right Knuckle	33
Figure 22: Old Brake Caliper(left), New mount(right).....	34
Figure 23: Manufactured Brake Caliper Mount Flush with Left Knuckle	34
Figure 24: Manufactured Brake Caliper Mount.....	35
Figure 25: Assembly of Manufactured Upper A-Arm Extrusion and Connecting Knuckle	37
Figure 26: Manufactured Tie-Rod Connection Piece Attached to the Knuckle	38
Figure 27: Wheel Knuckle with all Attachments Connected.....	39
Figure 28: Bracket Before Clearance was cut for nuts(left) and after(right)	40
Figure 29: Dimensions of New Handle Design	42
Figure 30: Comparison of Deflection in Handle Design	42
Figure 31: Orientation of Handles for Welding	43
Figure 32: Handle View on Assembled Rover	44
Figure 33: Exploded and Assembled View of Spectrographic Analysis Tool	45
Figure 34: Disassembled tool(left), assembled tool(right)	45
Figure 35: Pictures of Spectrographic Analysis.....	46
Figure 36: Instrument Deployment	47
Figure 37: Soil Sample Retrieval Tool	47
Figure 38: Solid and Liquid Sample Retrieval Tool	48
Figure 39: Full Solidworks Rendering of Wheel Assembly	49
Figure 40: Exploded Solidworks Rendering of Wheel Assembly	50
Figure 41: Finite Element Analysis Rendering in Fusion 360 on Hub Shaft Assembly	51

Figure 42: Exploded View of Wheel Hub Assembly	52
Figure 43: Wheel Hub Shaft Components with one Wheel Carcass	52
Figure 44: Pouring Polyurethane Rubber.....	55
Figure 45: Complete Rubber Tread	56
Figure 46: Solidworks Drawing of Hub-Foam Fixture.....	57
Figure 47: Shopbot Tool Path of Fixture	57
Figure 48: Fusion 360 Stock Orientation.....	59
Figure 49: Dimensions of Wheel Spoke	60
Figure 50: Solidworks Rendering of Final Wheel Assembly with Aluminum Spokes	60
Figure 51: Image of Carbon Fiber on MDF Fixture	61
Figure 52: Exploded Solidworks Rendering of Wheel Assembly	62
Figure 53: Fusion 360 Rendering of New Outer Foam Diameter	64
Figure 54: Wheel Pour Set Up.....	65
Figure 55: Final Assembly of Wheel	66
Figure 56: Inner Diameter of Hub Shaft Re-drilled to allow axle to fit through	67

Introduction

The space industry is made up of multiple different sectors and companies, but is primarily driven by the National Aeronautics and Space Administration, often known as NASA. Recently, NASA has focused its attention to Mars with the launch of the Perseverance Rover and hopes with the completion of a successful mission, this will be a stepping stone to landing humans on the Martian surface. With the development of NASA's Artemis Program, there is potential to have the first woman and next man to step foot on the lunar surface by 2024 and the goal to develop sustained human presence by 2028. In order to make a space travel mission successful, there becomes a demand associated with lunar exploration. Lunar rovers will increase the astronauts mobility to successfully explore and collect samples on the Moon. Annually, NASA hosts its Human Exploration Rover Challenge each year in Huntsville, Alabama challenging high school, college, and international teams to engineer the best rover suitable for traversing and completing various tasks on extraterrestrial terrains, similar to the lunar surface. This year, the Galileo Rover team will take part in the upcoming competition this April 2021.

During the competition, points will be utilized to determine the success of each obstacle and task. These points are obtained by completing various obstacles and tasks along a half mile course. In order to travel with the rover, NASA requires the design of the rover to fit within a 5'x5'x5' volume cube, simulating a lunar science payload and to weigh less than 210 pounds. Each rover must be human-powered, meaning the use of a motor or battery to improve drivetrain will automatically eliminate you from competition.

There are various design review requirements each team must complete throughout competition. On the first day of competition, the team must meet Mission Readiness Review Requirements (MRR) that will check for volume and weight constraints, the assembly's ability to

fold and unfold, as well as the clearance constraint. Judges will then complete an Excursion Readiness Review (ERR) before each course begins. This review will ensure each rider has proper attire and meets all safety requirements. During the competition, the course will have a total of 14 obstacles and 5 mission tasks for each team to compete for a maximum time frame of 8 minutes or less. There are 11 obstacles that have a voluntary bypass option. The 5 tasks consist of a spectrographic analysis, instrument deployment, core sample retrieval, solid soil sample retrieval and liquid sample retrieval. Each of the 14 obstacles consist of different levels of difficulty and include the following:

1. Undulating Terrain: wooden ramps that range from 6-12 inches in height with gradual ingress and egress slopes, all covered with gravel.
2. Crater with Ejecta: Large crater 3 feet in diameter with a vertical height of 8 inches, assembly covered by gravel
3. Transverse Incline: Angle of elevation incline is 20 degrees, no gravel
4. High Butte-Mountain Terrain: 5 ft high with a 20 degree incline before and after the peak
5. Large Ravine- Martian Terrain: 2-foot depression, about 8 feet wide
6. Sand Dunes - Martian Terrain: dunes are about 2 feet high and 3 feet wide at the base
7. Crevasses: Vary in width between 1 and 4 inches, cracks are 4-6 inches deep
8. Ice Geyser Slalom: Navigate to the bottom of the hill without coming in contact with any of the geysers
9. Lunar Crater: Asphalt lava with various size craters and strewn boulders testing the 12in clearance requirement

10. Bouldering Rocks: Navigate in field of asteroid debris (boulders), asteroid fragments range from 3-12inches
11. Tilted Craters: Travel up a slope and encounter a crater on the descending side, slope is 15 degrees
12. Loose Regolith: Beach sand pit with a depth of 6-8inches
13. Pea Gravel: Small bed of rounded pebbles at a depth of about 6inches
14. Undulating Terrain: Uneven terrain with humps on one side then the other designed to produce twisting forces on the chassis

In addition to earning points on each of the 14 obstacles, NASA also distributes awards for various other categories. Previous University of Colorado Denver Rover teams have won both the Featherweight Award and the Neil Armstrong Best Design Award. The Featherweight Award is awarded to the team that has the best innovative approach to addressing the current challenge of weight management in space exploration. The Neil Armstrong Award for best engineering design is no longer a part of the awards for this year's competition. In addition, there is also awarded an Overall Winner of the competition, which consists of being the top team in each of the following categories; design review, educational engagement, safety, and a successful excursion. There are another 10 awards given in addition to the ones mentioned above and these are; project review award, STEM engagement, social media, best team spirit, crash and burn, task challenge, rookie, pit crew and a few other various awards given based on the components of the competition. The Galileo Rover team seeks to win 1st place in the Overall Winner category and to bring home the Featherweight Award back to CU Denver.

Rider Selection

Introduction

It was important for the Galileo Rover team to confirm which two riders will be selected to navigate the rover during competition. This information can be used to determine the total weight of the riders with the rover in order to run analysis on the different components of the rover. The heights and dimensions of each rider are important in order to determine the position of the front and rear seats in relation to the pedals, as well as the placement of the handles and gearbox. The Galileo Rover team is currently working towards this completing this analysis.

Wellness Center Testing

In order to properly determine which two riders will be powering the rover, our team decided to accept Endeavour's analysis and complete rider testing in the CU Denver Wellness Center. Each member of the team completed recumbent bike testing by maintaining a specified RPM, which were the same as Endeavour and are displayed in *Table 1*. As each rider maintained the specified RPM and the resistance was increased until that RPM could no longer be maintained, once that took place it was lowered by one and the power output at this RPM was then recorded. Each rider having a consistent RPM allowed for a control in the testing as the resistance is dependent on the rider. The RPM's that were maintained during each rider's testing were: 70, 80, 90 and 100. This range was adopted from Endeavour as their analysis of the natural cadence of a cyclist determined to be sufficient. The power output, also called instantaneous power, is recorded in Watts and converted to ft-lb/s using the conversion of 1 Watt equal to 0.738ft-lb/s. The results from the testing are shown below in *Table 1*.

Rider	Power at 70 RPM (W)	Power at 80 RPM (W)	Power at 90 RPM (W)	Power at 100 RPM (W)
Aaron	250	267	236	250
Brooke	230	175	106	102
Evan	340	355	375	415
Hannah	320	275	290	378
Jaime	225	195	177	175
Kilian	340	353	371	418
Tolulope	147	213	153	154

Table 1: Instantaneous Power output acquired from recumbent bike testing

Power to Weight Ratios

The power to weight ratios are very important when determining which team member drives the rover during competition. Due to the team having a large variation of weights, it was expected that the power outputs would follow this trend. Therefore the team decided to use the average power output, compared to Endeavour who used the values at 80 RPM. This ratio was then calculated using the average power in Watts converted to ft-lb/s, with a combined rider's weight in pounds plus the weight of the rover, and once these two values were divided the final power to weight ratio is shown in ft/s in *Table 2* below.

Incline Climbing Velocity

In order to determine what the velocity will be while traversing up an incline, the same equations were used from the Endeavour rover team as a 20° incline was used. The 20° incline was used as it is the required obstacle incline during competition, each rover must be capable of traversing up and down the incline. The relationship between the rover and incline can be seen in *Figure 1*.

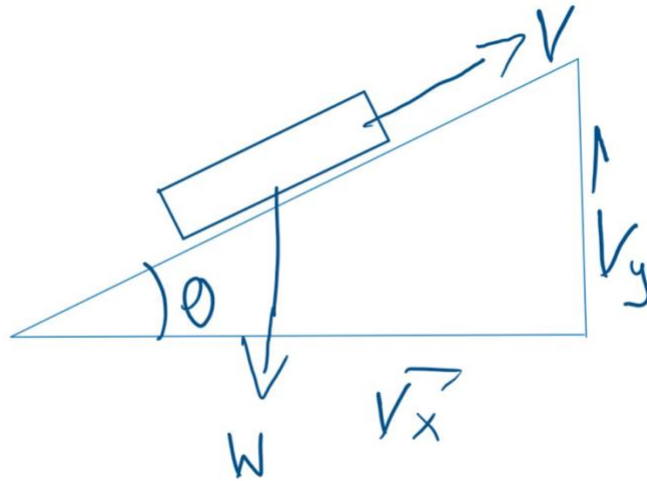


Figure 1: Free body diagram showing rover acceleration on an incline

In Figure 1, V is the velocity of rover traversing uphill, W is the weight of the rover and rider, θ is the degree of the incline at 20° and V_x and V_y are the horizontal and vertical velocities with respect to the triangle. The following equation was used to calculate the vertical climbing velocity in ft/s.

$$\text{Climbing Velocity} = (PW) / \sin(\theta) \quad (1)$$

This value used in Equation 1 was converted to a climbing velocity in miles per hour using the conversion factor of $1 \text{ mph} = 0.682 \text{ ft/s}$ and shown in Equation 2 below. This climbing velocity helped us determine the most suitable rider for competition and the results are shown in Table 2 below.

$$\text{Climbing Velocity (mph)} = \text{Climbing Velocity (ft/s)} * (0.682 \text{ mph}/(\text{ft/s})) \quad (2)$$

Rider	Average Power (W)	Average Power (ft-lb/s)	Rider Weight (lbs)	Weight of Rover + Rider (lbs)	Power to Weight Ratio (ft/s)	Climbing Velocity (ft/s)	Climbing Velocity (mph)
Aaron	250.75	184.95	158	318	0.58159	1.700	1.159
Brooke	153.25	113.03	121	281	0.40225	1.176	0.802
Evan	371.25	273.82	250	410	0.66786	1.953	1.331
Hannah	315.75	232.89	138	298	0.78150	2.285	1.558
Jaime	193.00	142.35	175	335	0.42493	1.242	0.847
Kilian	370.50	273.27	210	370	0.73857	2.159	1.472
Tolulope	166.75	122.99	225	385	0.31945	0.934	0.637

Table 2: Results of each riders power to weight ratio and climbing velocity

Results

The testing results show that Hannah and Kilian are the most suited riders for competition due to their high power to weight ratio and vertical climbing velocity. Now that this data has been gathered, it will be used to determine the seats and pedal placements on the rover which will need to be adjusted accordingly. It will also be used to determine the gear ratios for each rider. The team has decided the lighter of the two riders will be on the back of the rover but this assumption is subject to change.

Galileo Frame

Design

One of the main design objectives of the NASA Rover Challenge is to fit the rover within a 5'x5'x5' cube. In order for this to happen, part of the rover needed to be cut off and welded back on with allowing for a hinge mechanism to collapse the rear portion of the rover. The pedal mount was cut off and prepped to be welded with a hinge that will connect it back to the rovers frame. The hinge support folds back onto itself to fit inside the 5'x5'x5' constraint. Since the hinge support makes the pedal gear box unstable; the underside of the hinge support will be a locking pin. The locking pin mechanism was also welded onto the frame and the pedal mounts.

The hinge without the pin would not lock the rear of the rover into place, and would result in poor torsion being transferred to the belts. The hinge and locking pin were made out of aluminum that is welded to the aluminum frame. The hinges were made to be thicker than needed, this caused the aluminum to melt like butter when welded due to its thermal properties, therefore, the thicker the aluminum created a large weld puddle from the hinge down to the frame. The hinge part needed to be welded first so the locking pin pieces could be welded on with accuracy, in order to lock when the pedal and rear folding arm is folded out.

To reduce torsion in the frame, carbon fiber plates will be added to the frame of the Torsion plates. Three boards of MDF, with dimensions of $\frac{1}{2}$ 11 22 cubic inches each, were glued one on top of the other. The mold was then created by the shop bot following a program created in fusion, as shown in *Figure 3* below. Setting the MDF boards on the shop bot required the drilling of holes on all four corners and screwing the MDF boards to the shop bot table. Next, using the shop bot computer the location of the MDF board was established recognizing that the ball mill will be centered at the edge of the MDF boards. The shop bot will then form the plate tool using a $\frac{1}{2}$ inch ball mill. The mill will travel both ways in direction following an adaptive, horizontal, and parallel trajectory at a spindle speed of 1400 rpm. The cutting feed rate will be of 150 in/min and ramp feed rate of 10 in/min. The feed rate is slower for the helix ramp type for precision purposes. The ball mill will have a maximum ramp step of 2.5 inch, a clearance of .0413386 in, and helical and minimum ramp diameter of .475 inch.

Once the shop bot was finished, the torsion plate tool went through a post-processing stage to ensure that the torsion plates, created on that mold, will have a high level of accuracy. The post-processing included eight coats of oil based polyurethane being applied to the surface where the carbon fiber layout will be placed. At first, four coats were applied with a 10 minute

wait between coats. MDF can easily absorb the polyurethane, there for 4 coats where required to ensure enough of the polyurethane remains and dries on the surface. Thereafter, the tool was smoothen using a P-400 grit grade sandpaper. The sanding process was performed after each new coat of polyurethane had dried off; starting after the fourth coat polyurethane was applied, and finishing after the eighth coat was applied. This will achieve a crater less and uniform surface, seen below in *Figure 2*. The final post-processing step of the plate tool was to use a polishing compound and the buffing wheel drill to polish the surface of the plate tool.



Figure 2: MDF Torsion Plate Mold

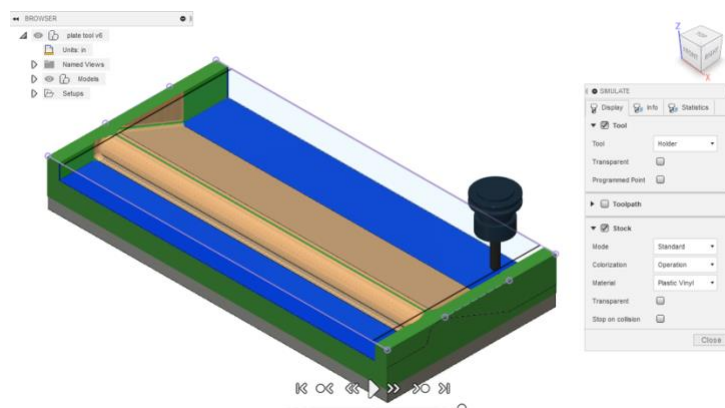


Figure 3: Torsion Plate Mold from Fusion 360

The plate tool was able to form two halves of one torsion plate at a time; reducing the time needed to form two torsion plates, and reducing the amount of carbon fiber material that was wasted while creating the plates, seen below in *Figure 4*. The Pre-layout required materials such as skin protective gloves, paper towels, peel ply, breather cloths, vacuum bag, clear resin, hardener, measuring cups, mixing sticks, spreader, carbon fiber sheet, and zyvax. The first step was to create a template with the measurements of the surface that will be occupied by the carbon fiber material; which covered an area of 10 inches by 22 inches. Using this template, it was determined a piece of 1 foot 10 inches by 8 feet was required to form each torsion plate. This piece of carbon fiber sheet provided the material needed to reach a part thickness of .10 inches; the thickness required for a SF of 4 of the torsion plates as shown in *Figure 5*. Next, using paper towels, Five coats of zyvax composite shield mold release was applied to the surface where the carbon fiber sheets will be laid. There was a 15 minute wait between each coat to ensure the zyvax agent was fully dry after each coat. Thereafter, the breather cloth and peel ply sheet were cut to cover the area of the torsion plate template. The fourth step was to cut a piece of the vacuum bag to enclose the volume of the torsion plate. At the same time a piece of bag was cut to enclose the previously mentioned carbon fiber sheet; 10 template markings were created along the surface area of the bag, to mark where the bag and carbon fiber sheet will be cut. After the materials are all set up the carbon fiber layups can be started.

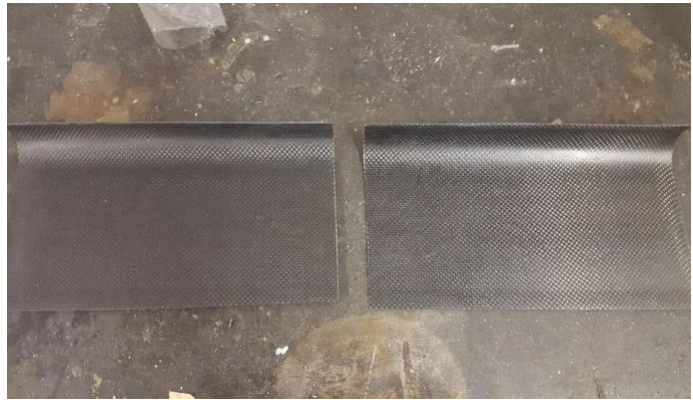


Figure 4: MDF Torsion Plate Tool and Carbon Fiber Plates

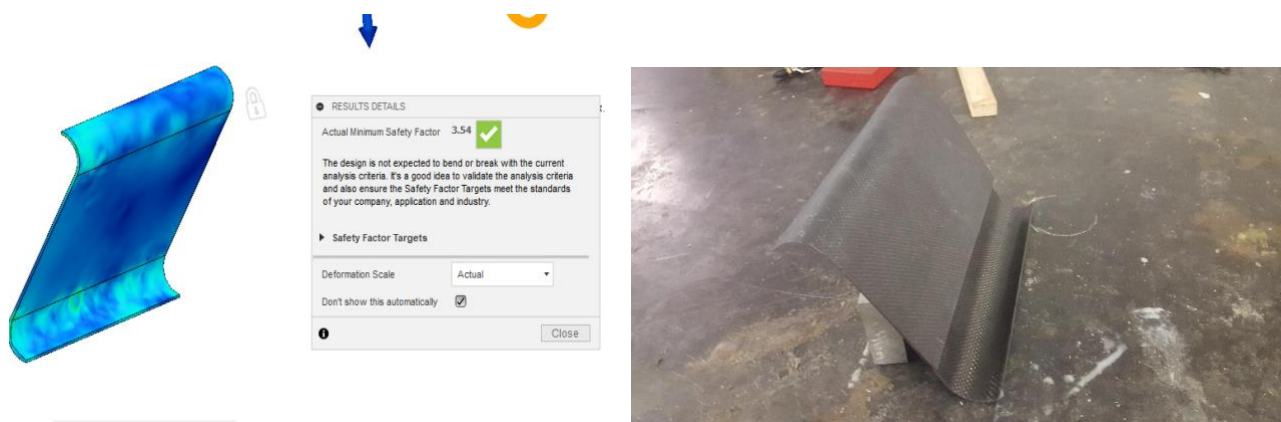


Figure 5: "S" Torsion Plate and Manufactured Carbon Fiber Torsion Plate

Ten pieces of carbon fiber sheet, the size of the template, were used to form the torsion plates on the torsion tool shown above in *Figure 5*. The first step to begin the layout was to calculate and measure the amount of resin and hardener required by the amount of carbon fiber being used. The resin to hardener ratio was calculated to be 150 g of resin to the 75 g of hardener for the carbon fiber sheet. The mixture was then added to the carbon fiber sheet that was enclosed in the vacuum bag. Using the spreader the chemical mixture was evenly spread throughout the carbon fiber sheet inside the vacuum bag. The carbon fiber sheet was then cut into 10 pieces . These pieces were placed on the plate tool one at a time. Afterwards, the piece of peel ply was cut into smaller strips that will cover the carbon fiber by overlapping each other. This same process was done with the piece of the breather cloth cut during the pre-layout; the breather cloth pieces

were laid on top of the peel ply shown on the left in *Figure 6*. The purpose to overlap the peel ply and the breather cloth was to allow for any air left in the set up to circulate once the vacuum pump was attached. The final step of the layup was to bag the tool and set the vacuum pump shown on the right in *Figure 6*. The purpose of the vacuum pump in the setup is to draw out the air from the layup and provide the pressure needed by the peel ply to reduce contamination of the patch surface by uniformly removing excess resin and hardener mixture from the carbon fiber; increasing the part accuracy. Not to mention, the pump will help any air molecules that may leak through the pipe connection, to circulate with the help of the breather cloth. Bagging the carbon fiber layup and the mold required sealant tape with contours on each side to compensate for the round feature on the higher section of the plate tool. The pump was then attached to the setup and it reached a pressure of over 20psi. Once the Vacuum pump is attached to the set the about 8 hours will pass before the resin and hardener have dried in the carbon fiber.



Figure 6: Breather Cloth & Peel Ply, Vacuum Bagging of Carbon Fiber Layup

After 8 hours the resin and hardener mixture has dried in the carbon fiber and the part can be removed from the plate tool. However, the curing process may differ depending on the pressure being exerted from the vacuum pump on the layup. Moving on, The post-processing of the torsion plate was fairly simple. The first step was to trim the excess carbon fiber surrounding the part

using the bandsaw. No measurements are required for this cut, as only excess material is being removed. The next step was to sand all the edges, using a sand paper of P-320 level grit, while continuously using a square tool to ensure the part's edges are as precise as possible. Once these steps were done, the midpoint of the part was marked with a line and the plate cut in half using the bandsaw; the newly formed edge was also sand down for part quality purposes. By the end of the process two sets of half torsion plates were produced for the frame of the rover.

The two sets of half torsion plates will be adhered using the EA 9309 epoxy adhesive. Two halves were adhered at their mid-sections increasing the thickness of the torsion plate. At an area of about 4 inches tall by 9 inches wide the overall thickness of a single plate is two thousandths of an inch; which will double the overall safety factor of the torsion plate. Moreover the torsion plates were attached to the rover frame using the EA9390, in the mid-section of the rover under the riders seats. This position was determined by the force simulation performed on fusion; which showed that the frame stringers will experience the highest amount of stress at the midpoint between the two seats. The torsion plates will reduce the torsion in the frame as well as support the mid-frame structure, seen below in *Figure 7*.



Figure 7: Frame and Suspension Assembly(left), Torsion Plates under Seats(right)

Seats

Taking into consideration the success of the Odyssey Rover and our limited budget, the seat design will consist of the same ergonomic and modular foam shown in *Figure 8*. The seat foam will be attached to the already built carbon fiber seat frame for weight reduction. The seat frame was made out of carbon fiber seat to ensure that the rider does not fall out of the rover as it is maneuvered in un-even terrain. These seats will be attached to the frame of the rover using four aluminum pipe clamps per seat. The clamps wrap around the stringers of the frame, using a rubber gasket to protect the stringers from damage. The clamps will be bolted to each other not to the stringers. This will allow for the seat placement on the frame to be adjusted depending on the height of the riders. The seats will be leaning on each other with the help of an H shape seat support. In addition, the seats will include the 4-point harness type seat belts . These seat belts will be attached to the stringers of the frame. Ensuring the passenger’s safety as the riders will be held in place by the weight of the rover, instead of the structure of the seats.



Figure 8: Seats Attached to the Frame(left), Seat Foam & 4-point Seat Belts(right)

Suspension

Regarding the front suspension of the rover, the design of the A-Arms did not change. However, the fox float air shock settings were adjusted for the suspension to function efficiently. Taking into consideration the weight of the front rider, the air pressure in the shocks were adjusted to 140 psi for rebound using the air shock pump. This pressure adjustment along with the position lever to “Mid” will allow the shocks a max travel of about 1.75 inch, giving the shock a sag of about .53 inches. Setting the position lever to “Mid” on the air shocks will allow the shock to be rigid enough to sustain the weight of the front section of the rover; reducing the amount of forces that reach the frame, without fully compressing under the weight of the rover and the rider. The setting of the suspension shocks were adjusted once the front suspension was assembled on the frame of the rover seen below in *Figure 9*. For the rear suspension, the pressure adjustment for the single shock was lower than the front suspension shock settings. Taking into consideration that the rear section of the rover weighs less than the front end of the rover, and that the lighter of the two riders will be sitting in the rear section of the rover. The air pressure in the rear shock was set at 120 psi for rebound. The shock will be at an “Open” setting and will have a travel of about 1.5 inches allowing a sag of .45 inches. Moving on, with the two gear belt system of the rear drivetrain shown in *Figure 10* below, the tension of the belts located on the rear pedal post and rear suspension stud will not be affected by any movement on the suspension. Setting the position lever to “Open” will allow the shock to be the least rigid; allowing the shock to react to forces while being subjected to the lower weight of the rear section of the rover. The settings of the shock were adjusted once the rear suspension was assembled and attached to the frame of the rover.



Figure 9: Front Suspension Assembly

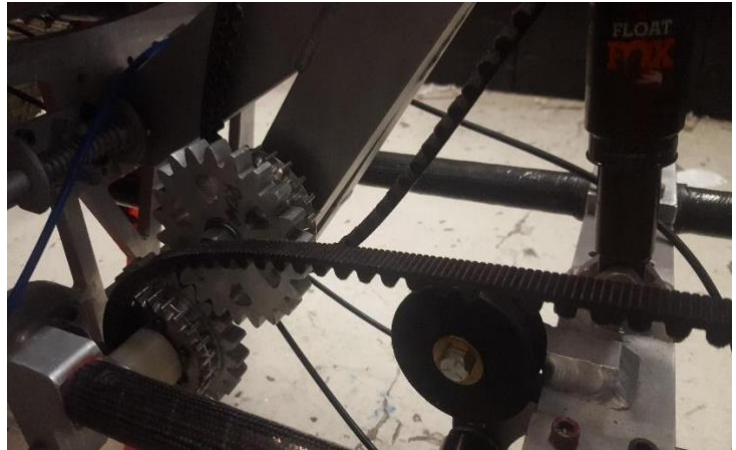


Figure 10: Rear Suspension Assembly(left), Two-gear Belt System (right)

Specific upgrades on the rear suspension include the rod that will be used as the pivot point. The rod was replaced by a hollow rod after consulting with Professor Cullen. A hollow rod was determined to have higher torsion stress tolerance, than a solid bar of the same mass according to the polar moment of inertia. However, with an increment of the rod's outer diameter from $\frac{1}{2}$ an inch to $\frac{3}{4}$ of an inch pipe as shown in *Figure 11*. Increasing the size of the stud, required the resizing of suspension components, a drive train gear, and frame inserts that depend on the suspension rod for support.



Figure 11: New Hollow Rod(left) and Solid Rod(right)

However, FEA simulations were performed to determine that the resizing of the rear suspension pivot components will maintain a safety factor of 3. This can be seen in *Figure 12*. The Stringer inserts, rear control arm inserts, and the rear pedal post holes were all resized to fit the tube. The stringers insert holes were resized using a fusion program in combination with the end mill to achieve the best precision possible for the circumference. The stringer insert was placed inside the CNC mill machine on its flat side. The next step was to locate the position of the part inside the Haas T2 CNC Mill, as well as the center of the insert hole, and uploaded the information to the CNC Mill database. Thereafter the fusion program that consisted in creating a one-inch

diameter hole, with a $\frac{1}{2}$ inch flat end mill, was uploaded to the machine. The end mill required a spindle speed of 4583.66 rpm and a feed rate of 13 in/min. A clearance height from retract height of .4 inches, A retract height from stock up from .2 inches, and a feed height from top height of .2 inches. The flat end mill will perform a total of 3 finishing passes with a maximum roughing step down and a finishing step down of .125 inch. All this with a tolerance of .004 inch. The inserts were resized, to a 1-inch Diameter, to fit a copper fitting with an inner diameter $\frac{3}{4}$ of an inch shown in *Figure 13 below*. The 1-inch copper fitting has an inner diameter of $\frac{3}{4}$ of an inch and it is required inside the stringer insert to enable the 4130-steel tube to rotate on its x-axis with least amount of friction. This will allow the rear suspension to pivot efficiently when needed. The same procedure was performed for resizing the gear located on the rear suspension stud. The center location of the hole was located by the CNC mill, and then the fusion program to resize the hole diameter was uploaded into Haas mill software. However, the only difference in program being that the flat end mill will travel 6 hundredths of an inch less, and will only be required to perform one finishing pass. After the procedure in the Haas CNC mill was done, a bronze bearing was also introduced in the bearing using the press. The bronze bearing will allow the gear to rotate on the 4130 steel stud with the least amount of friction possible; allowing the rear drive train of the rover to perform without difficulty.



Figure 12: Rear Suspension Pivot Components on Fusion 360

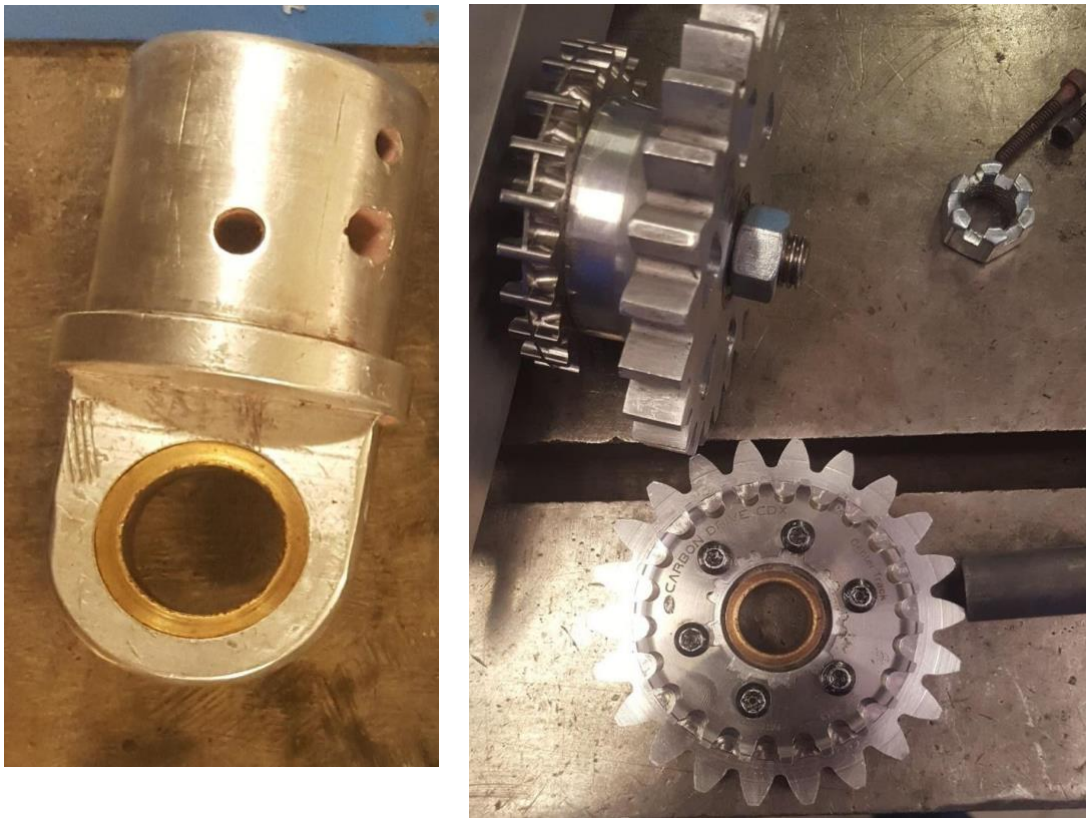


Figure 13: Stringer Inserts with brass fitting(left), Drive train gear with brass fitting(right)

Moreover, the holes for the pedal post and the holes for the rear control arms were resized using a combination of a $\frac{3}{4}$ inch drill and a reamer. In this case the Vectrax machine was used to reduce time required to resize the holes to $\frac{3}{4}$ inch. These holes did not require any fittings, therefore the procedure to resize did not require the CNC mill to increase the precision of their circumference. First, both the pedal post and the suspension arm inserts were adjusted and maintained flat on the bed of the Vectrax mill; one part at the time. Second, the center of the holes in the pedal post and in the suspension arm inserts were located with the $\frac{3}{4}$ of an inch drill bit. Next, the speed of the mill was set on LOW at about 190 rpm. You will then pull the drill up and down slowly to get rid of the shavings, until the drill goes all the way through the hole. The final step will be to substitute the drill bit with a reamer of the same size to get the smooth hole surface. Afterwards the all the parts were assembled on the rear suspension, and the rear suspension was attached to the frame, as shown in *Figure 14* below.



Figure 14: Photo of Suspension with Torsion Plates Attached to Frame

Galileo Drivetrain

Gear Ratios

Unlike the previous semester, the gears used to link the gearbox and the driveshaft have been referred to as sprockets this semester. This reflects the naming convention used by Gates Carbon Drive, especially since they attach to a belt instead of each other. The components inside the gearboxes are still referred to as gears. For this report, gear ratios will refer to the gears inside the gearboxes while the final drive will refer to the sprockets.

While looking for the sprockets at the machine shop, the characteristics of the rover's drivetrain were discussed. Both riders have a set of pedals that attach to their own Pinion C1.9 gearbox. For each rider, the output of the gearbox is attached to a sprocket. For the front rider, the sprocket is linked to another sprocket fixed to the front drive shaft using a belt. For the rear rider, who faces the opposite direction of the front rider, the sprocket is linked a pair of reversing gears using a belt. The reversing gears are linked to another sprocket fixed to the rear driveshaft using a different belt. This allows for both wheels to rotate the correct direction despite the gearboxes facing opposite directions. The sprockets and belts are provided by Gates Carbon Drive, and the reversing gears were manufactured by the 2017-2018 Odyssey Rover team.

Proper analysis of the drivetrain allowed for the final drive to be calculated. Because the gear ratios inside the gearboxes and the sprockets attached to the gearboxes cannot be changed, this can only be done by changing the sprockets attached to the driveshafts. The procedure we planned to use in the previous semester was changed slightly to account for updated list of constants, known variables, and unknown variables. Before any calculations were made, all variables and constants were converted to a standardized set of units. All length measurements, except for the sprockets' radii, were expressed in feet. Gates Carbon Drive uses the number of

teeth to label their sprockets, so the radii are substituted for the number of teeth. The surface angle was expressed in radians while angular velocity was expressed in radians per second. This is consistent with how angular velocity used to calculate tangential velocity. Last semester, there was a mistake with this conversion such that it defined the relationship between rpm and radians per second to be 0.209 instead of 0.105. This has been corrected. Weight was expressed in pound-force, so power was expressed in foot pound-force per second.

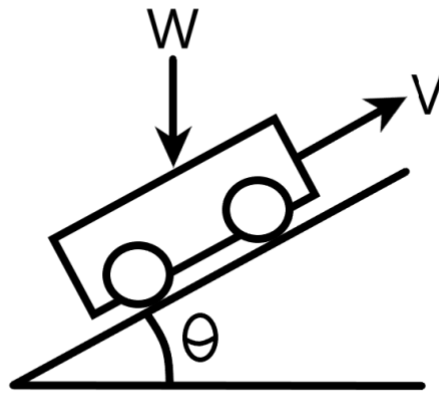


Figure 15: Free Body Diagram of Rover on Incline

To calculate the velocity of the rover, the dynamics equation for power was derived from *Figure 15* and rearranged so that it was expressed in terms of force and velocity. Because the only unknown variable is velocity, the equation can be rearranged again. The velocity of the rover was calculated using Equation x1 in Appendix H. With the velocity and the known radius of the wheels, the angular velocity of the wheels could be calculated using a tangential velocity equation derived from *Figure 16*.

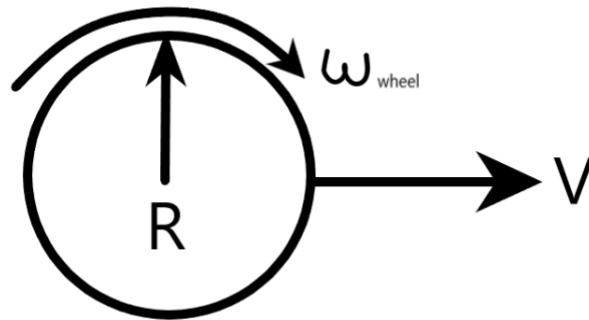


Figure 16: Free Body Diagram of a Wheel on the Rover

The angular velocity of the wheels was calculated using Equation x2 in Appendix H. Because the angular velocity of the wheel is equal to the angular velocity of the drive shaft sprocket, notated using 2, this can be compared to the angular velocity of the gearbox sprocket, notated using 1. Calculating the angular velocity of the gearbox sprocket requires the angular velocity of the pedaling and the gear ratio selected inside the gearbox. We assumed that the riders will pedal at an angular velocity of 70 rpm to maximize power efficiency. Knowing the gear ratio of the lowest gear and the angular velocity of the crank, the angular velocity of the gearbox sprocket was calculated using Equation x3 in Appendix H.

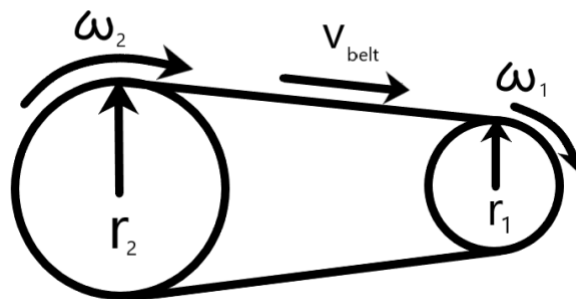


Figure 17: Relationship Between Input Gear and Output Gear

The final drive was calculated using the equations derived from *Figure 17* and Appendix H. Using the final drive and the number of teeth on the gearbox sprocket, the number of teeth required on the driveshaft sprocket was calculated using Equation x5. Based on these calculations, the drive train sprockets should have 70 teeth. With the 32 teeth sprockets on the gearboxes, this gives a final drive of 2.2. We do not have sprockets with 70 teeth, so we must order them.

After the final drive was calculated, the equations were rearranged, setting velocity and surface angle as the unknown variables. The Pinion C-Line Manuel only lists the first and last gear ratios. To get all 9 gear ratios, an external site had to be used. This site reversed the gear ratios such that the lower gears had a lower value than the higher gears. These values had to be inverted when performing these calculations. This allowed us to plot the velocity with respect to surface angle for each gear. The velocity was converted to miles per hour for these calculations and a graph of their relationship can be seen below in *Figure 18*.

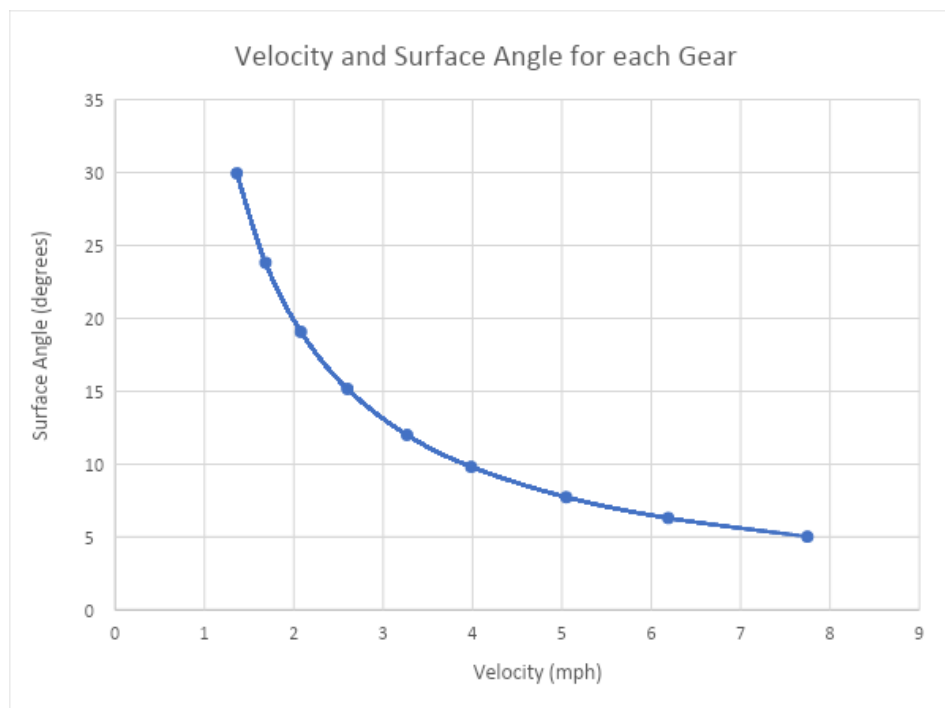


Figure 18: Relationship between the Surface Angle and Velocity

The position of the gearboxes and seats must be decided. This will depend on the length of the belts available to us and the dimensions of the riders. It would be optimal to position the seats as close to the center of gravity as possible to improve stability.

After calculating the appropriate final drive for the rover, the next step was to order the necessary parts. After inspecting the rover and the available parts in the shop, it was decided to use the parts in the shop instead of ordering new ones. The driveshafts use a specific mounting style, and it was initially unclear which type of sprocket could be attached to the driveshaft. After reviewing the work of previous teams, as well as looking at the available parts in the machine shop, it was determined that the rover used two 22 teeth, 9-spline/6-bolt CDX rear sprockets. The combination of 9-spline and 6-bolt attachments was chosen by previous teams to match the 6-bolt mounted brake calipers. This mounting style is only available with 22 teeth sprockets. There was not adequate time to redesign the driveshafts to use a different mounting style, so these sprockets were used in the final assembly. For the gearboxes, one of them had a 32 teeth Pinion CDX:SL front sprocket attached. This is the sprocket that was planned to be used for both gearboxes, so the CDX:SL was kept in the gearbox for final assembly. The other gearbox did not have a sprocket attached. Whichever sprocket was selected had to have a 4-bolt mounting style as opposed to the Pinion mounting style. The smallest compatible sprocket available in the shop was a 39 teeth, 4-bolt CDX front sprocket. This is the smallest 4-bolt sprocket available from Gates Carbon Drive, so the 39T CDX from the shop was used for final assembly.

Gear Selector

One of the gearboxes did not have a gear selector attached. This gear selector and its pieces were found disassembled. The initial plan was to repair and install the gear selector in the

shop. Some components were missing or damaged. This included M1.5 set screws and the cable pulley. These parts were not found while looking online or in bicycle stores. A decision was made to instead order a new gear selector. Gates Carbon Drive does not offer direct orders or shipping, referring to online distributors to order any parts. The gear selector as an independent part was not listed either as an option to order on online stores. A bicycle shop carried rotary shifters from other brands, including a 9-speed. An assumption was made that if the gear selector was compatible with a 9-speed gearbox, it would be an acceptable replacement. After reviewing the replacement, it was discovered that Gates uses a unique rotary gear selector that loops the wire back into the handle. The decision was made to assemble the rover without the gear selector.

Galileo Steering

Steering Design

The main goal for the steering team this semester was to finalize the last pieces needed for manufacturing and get the handles welded before assembling all parts. The steering design consisted of two pitman arms, one of which was offset from the front bulkhead by a five-inch aluminum bracket. The handles were connected in a linear fashion to the end of each pitman arm and two tie rods were attached to the top pitman arm, connecting the steering system to the front wheel knuckles. The tie rods were used to translate the linear steering of the handles into angular direction for the wheels. *Figure 19* and *Figure 20* show a top down view of the assembled steering design and a back view, respectively.

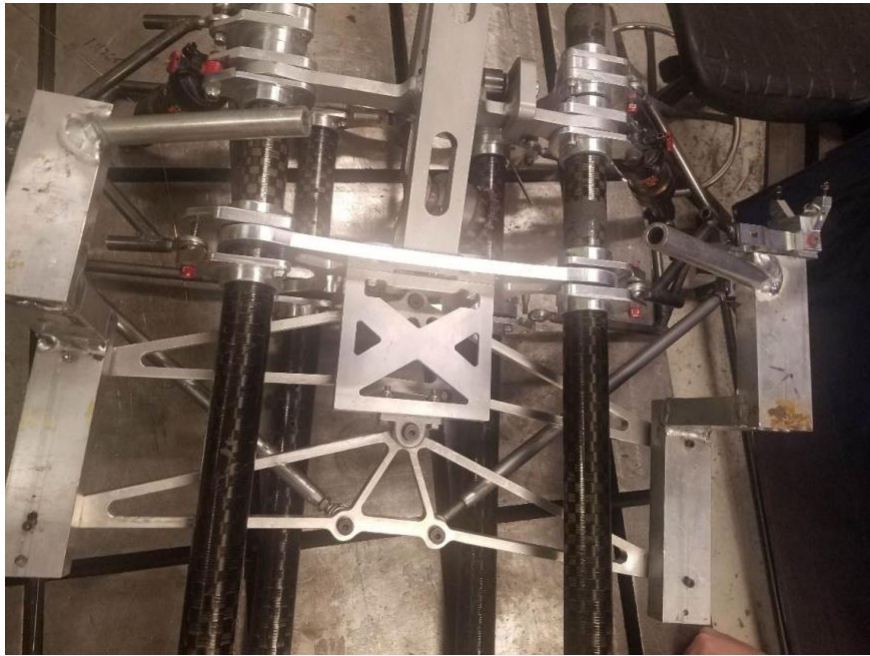


Figure 19: Top down view of steering design assembly with handles



Figure 20: Back view of steering assembly



Figure 21: Close up of Tie Rod Connection Top Pitman Arm to Right Knuckle

Caliper Mount

After machining the knuckles last semester, it became evident that the previous caliper mounts would be incompatible with the new knuckle design. The centerline for the two pieces did not line up and the connecting angles were off as well. In addition to this, there was no piece designed or already manufactured for the right caliper mount. A new design was created to solve these problems, and a comparison of the old versus new caliper mounts can be seen in *Figure 22*. Originally, the mount was designed to fit flush along both the right and left sides of the knuckle, however the stock chosen for the piece was fractionally too short so 0.3 inches was removed from the far edge. The final design and manufactured piece can be seen in *Figure 23*.

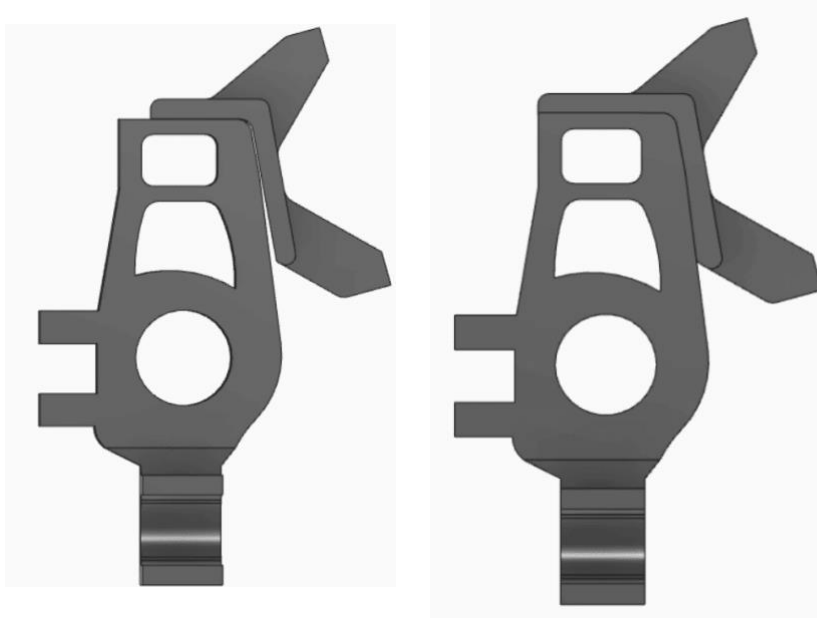


Figure 22: Old Brake Caliper(left), New mount(right)



Figure 23: Manufactured Brake Caliper Mount Flush with Left Knuckle

The brake caliper mounts were manufactured on the CNC and Vectrax Mills out of aluminum 7075. The CNC process took 4 operations with 3 tool changes. The stock was placed face up and a $\frac{3}{4}$ " flat end mill carved a rough outer profile of the designed piece. This was done using multiple depths and 4 roughing passes. Next a $\frac{1}{2}$ " flat end mill was used to finish the outer

profile with multiple depths of 0.5 inches. A ¼” flat end mill was chosen to finish the inner curvature that sits flush against the knuckle with the tool machining at multiple depths of 0.2 inches. The last tool change was made back to the ¾” flat end mill in order to machine stock down from the top of the piece to the top of the brake teeth. This was done using multiple depths and 2 roughing passes.

After the main profile was finished in the CNC mill, the mounts were brought to the Vectrax mill. There was some trouble arranging the part to be held firmly within steel jaws to drill the center hole. Eventually the part was placed with the brake teeth hanging off the edge and parallels placed under the top hood, with clearance for the center hole to be drilled. The center hole location was marked off before a center drill was placed to begin a groove at the correct location, finally the 3/8” drill bit was placed to drill the hole. The part was then turned onto its side with parallel bars being used to ensure the edges of the caliper teeth were parallel with the drill bit. These holes were tapped for a M6x1 drill, first using a center drill before tapping the holes. The process took time as the tap drill was required to repeatedly withdraw so as not to clog the hole or break the drill bit. A fully manufactured and drilled caliper mount may be seen in *Figure 24*.



Figure 24: Manufactured Brake Caliper Mount

Upper A-Arm

The upper a-arm extrusion was made out of aluminum 7075 and machined on the CNC and Vectrax mills. The machining process was a relatively simple one with only 2 operations and 1 tool change. The stock was placed in the machine so that once finished, the opening of the double shear connection would be facing up. A $\frac{3}{4}$ " flat end mill was used to do a rough outer profile of the arm using multiple depths and 4 roughing passes. A $\frac{1}{2}$ " flat end mill was then used for a final smooth outline, using multiple depths of 0.4 inches.

The part was then moved to the Vectrax mill where it was held between steel jaws along its greater length with the double shear connection hanging over the edge, and the thin excess material facing up. A $\frac{1}{2}$ " drill was used to shave off a thin 0.01 inch "top hat" of material. After confirming the desired width of the piece at 0.9 inches, the part was placed back within the Vectrax along the same length but with the double shear connection facing top down to drill the center holes. A center drill was used to mark the hole along the top connection before being replaced by a $\frac{3}{8}$ " drill. Once the drill passed through the top connection, the center drill was replaced to mark off the hole along the top of the bottom connection. The $\frac{3}{8}$ " drill was replaced once more to drill through the end of the piece. The part was then turned around, so the steel jaws clamped along the double shear connection. A center drill was used to mark the center hole, and a $\frac{3}{8}$ " drill was once more used. Due to the thickness of the part, the drill had to be withdrawn a number of times so as to avoid clogging the hole. At one point the part began to move slightly as the drill was pressed so a piece of rough sandpaper was placed between the jaws and the part to hold it steady. After the holes were drilled, the final step was to fillet the outside edges so as to fit within the designated hole within the knuckles. Through a process of flattening, curving, and dunking in water to cool the metal, the edges of the long arm were filleted about an

inch along the length using the grey wheel. A final assembly of the upper a-arm extrusion connected to the knuckle may be seen in *Figure 25*.



Figure 25: Assembly of Manufactured Upper A-Arm Extrusion and Connecting Knuckle

Tie Rod Connection

The tie-rod connection piece was redesigned shortly after manufacturing of the upper a-arm extrusion was finalized. The original design lacked any sort of parallel edges which would have complicated the machine process, specifically while drilling holes. The part was also longer than needed for the tie-rod connection. We ran into two problems while machining the first connecting piece. The first issue being that a $\frac{1}{4}$ " flat end mill was chosen to machine a 1.168 inch deep part which ignored the 3:1 rule when choosing thickness of tool to depth of part. The issue was caught before doing any permanent harm to the piece. The operation requiring said tool was completed using 3 step-downs so a longer drill bit was used to successfully complete the operation. The second issue was discovered after the part was completed and it was revealed

that the double shear connection was 0.016 inches too thin. The design was edited on Fusion 360 and the necessary operation was resent to the CNC mill to widen the connection.

The full process on the mill took 4 operations and 3 tool changes. The stock was placed so that once complete, the extruded piece and double shear opening faced up. The first operation was made with a $\frac{3}{4}$ " flat end mill along the outer profile of the part. This was completed using 2 stepovers and multiple depths. Next a $\frac{1}{4}$ " flat end mill was used to smooth out the profile using 3 stepdowns at 0.4 inches at a time. The $\frac{3}{4}$ " flat end mill was returned to shave away bulk material along the top of the double shear opening. This was completed using 3 passes and multiple depths. Finally a $\frac{1}{4}$ " ball end mill was used to generate a ramp along the connecting edge of the shear connection using a stepover of 0.025 inches. The finished connecting piece may be seen in in *Figure 26* and *Figure 27*.



Figure 26: Manufactured Tie-Rod Connection Piece Attached to the Knuckle



Figure 27: Wheel Knuckle with all Attachments Connected

Steering Bracket

The 5-inch connecting bracket underwent a few design modifications before the machine process could begin. The original part included extra cuts within the piece to help lower the weight. These cuts would've made machining more complicated and with the priority of the featherweight award being passed over, the choice was made to remove those cuts to both speed up production and assembly of the rover.

The bracket was machined on the Haas TM-2. Stock was chosen of nearly exact width necessary and plenty of excess length and width. The stock was clamped using four toe clamps along the edges, with the program marked off at the center of the stock. The machine process took 5 operations and 2 tool changes. To begin a ½" flat end mill was used to carve out the inner pocket of the bracket, using multiple stepovers and stepdowns. Next, that same tool was used to do a rough outline of the cuts within the pocket, using a rouging stepdown of 0.55 inches. The tool was changed to a ¼" flat end mill to smooth out the pocket cuts using multiple depths of 0.1

inches. The tool was switched back to a ½” flat to do a rough outline of the 5”x5.5” box. This was done using multiple depths of 0.15 inches and leaving triangular tabs along each edge. The same tool was used to do one final smooth pass along the outside, leaving the tabs intact.

The part was then taken to the slot machine where stock was cut along the tabs to separate the main design piece from the remaining stock. The bracket was moved to the Vectrax and set within steel jaws, along parallel bars so that each of the four tab locations could be accessed at the same time. A ½” drill was used to work along the outside edge of the bracket and remove the jagged edges remaining of the tabs. Lastly the edges were smoothed along the grey wheel.

The final part of manufacturing for the bracket was to be drilled for connecting holes to the bulkhead and pitman arm. It was placed upright in the Vectrax so a 3/8” drill could drill two holes to connect the bracket to the bulkhead. Then it was flipped 180° and two ¼” holes were drilled for the piece connecting the bracket to the pitman arms. Once the holes were drilled, it was realized that there was not enough clearance room for the nuts at the end of the 3/8” bolts to screw on, so the bracket was once more placed on the Vectrax mill and a crude outline was cut to allow clearance space. The finalized bracket can be seen in *Figure 28*.



Figure 28: Bracket Before Clearance was cut for nuts(left) and after(right)

Path Forward

Assembly of the steering design was completed in shifts as the original connecting tie rods were exchanged for slightly longer ones and attached to the upper pitman arm instead of the lower. This was due to the shorter ones being unable to push the wheels at the full necessary angles. After the handles were welded, they also needed to be re-drilled before they could be attached to the steering system. The final steering design succeeded in allowing the driver to steer in a linear fashion while translating the directions into angular motion for the wheels.

Due to certain time and personnel constraints, there was very little time to test the steering model outside of CAD simulations. For future teams looking to improve this model, the primary concern should be on stability. The parts connecting the lower pitman arm to the front bulkhead and the upper pitman arm to the bracket were both made with single shear designs. While the steering system is functional, the connections are less secure due to this. The other focus could be on the handles. Once fully assembled the handles sat at a lower height than anticipated. At the current fit, they sit low enough that the driver may have to constantly be leaning forwards to have a decent grip on the handles.

Handle Design

After conversing with Doug Gallagher and Kevin Fornall, it was decided that the handles were not sturdy enough for competition. New handle mounts were designed from two inch by one inch, one eighth inch thick aluminum 6061 tubing. *Figure 29* below shows the dimensions of the new handle design.

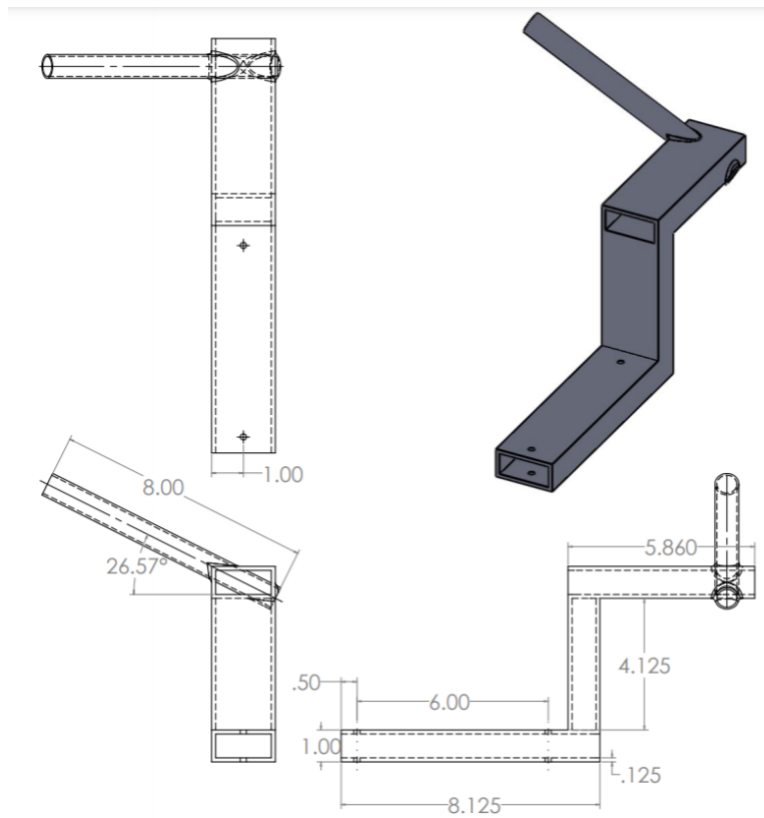


Figure 29: Dimensions of New Handle Design

In addition to changing the tubing sizes, the handles now go through the entire tube instead of being welded to the surface of one side. These changes increased the weight of each handle by 0.13 pounds but reduced the deflection of the handles by 84%. Figure 30 below, shows a comparison in the deflection of the two handle designs.

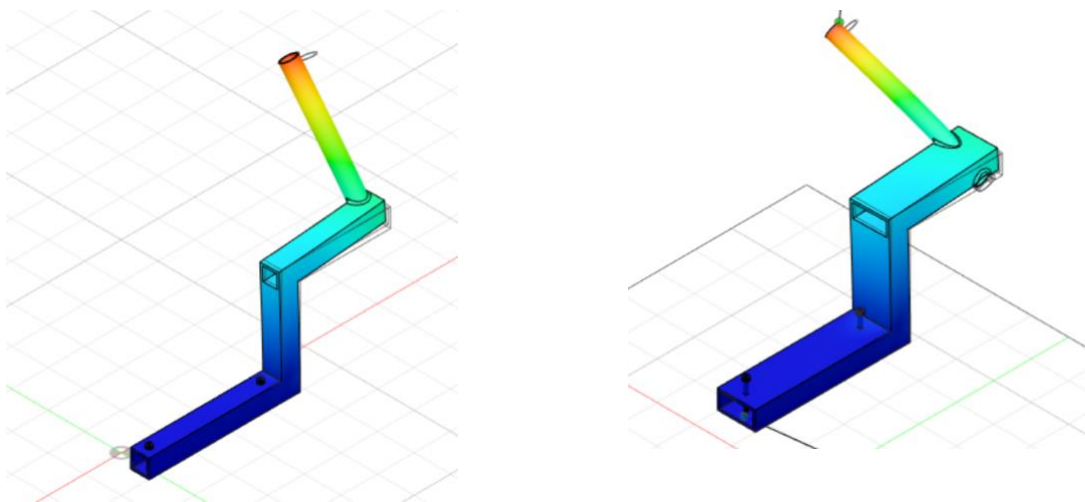


Figure 30: Comparison of Deflection in Handle Design

These deflections were calculated in Fusion 360 with a forty pound load applied to the handle to simulate our maximum required turning force on the handles. The maximum stress on the first handle design was 84.4 MPa and the maximum stress on the current design is 15.5 MPa. The reduction of stress allows for increased durability of the handles and gives extra room for error on the reaction forces from the seat caused by steering.

To manufacture the new handles, six lengths of tubing were cut from stock with a band saw. Edges of these pieces were cleaned up with a disk sander to reduce sharp edges. Two holes were drilled into each of the 8.125" lengths for mounting onto the pitman arms. These holes were drilled with a 0.1935 diameter bit on a drill press and then deburred. The two 5.86 length tubes were placed in the mill to drill a 0.750 inch diameter hole from opposite corners of the tubing. The stock was placed into an angle vice fitted to twenty six degrees and then a probe was used to find the correct coordinate system within the mill. A five eighths inch end mill was used to create the holes for the handles. After being removed from the mill, both rectangular tubes were deburred and sanded to allow for easier insertion of the handles.

Then, all four components of each handle were welded using an AC Tig welder. *Figure 31* below, shows the orientation that the pieces were welded in.



Figure 31: Orientation of Handles for Welding

The handles are currently mounted on the completed rover as shown below in *Figure 32*. After assembly, we realized that the upright arm of the handles was too short and did not allow room for the rider's legs to sit between the handle and the seat. Future teams will need to reconstruct the handles with an upper arm approximately 4 inches longer.



Figure 32: Handle View on Assembled Rover

Tasks

To complete the spectrographic analysis task, a tool was designed to attach to the driver's phones. This tool has a dial with four slots that will be positioned in front of the phone's camera. Three of the dials contain a photo-filter and one will remain empty. This allows the drivers to take three filtered and one unfiltered photograph of the target and upload them to the judges.

Figure 33 below shows an assembled and an exploded view of the tool.

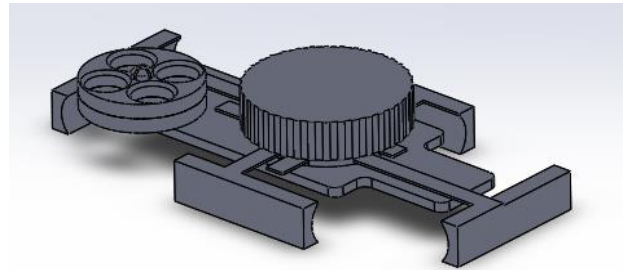
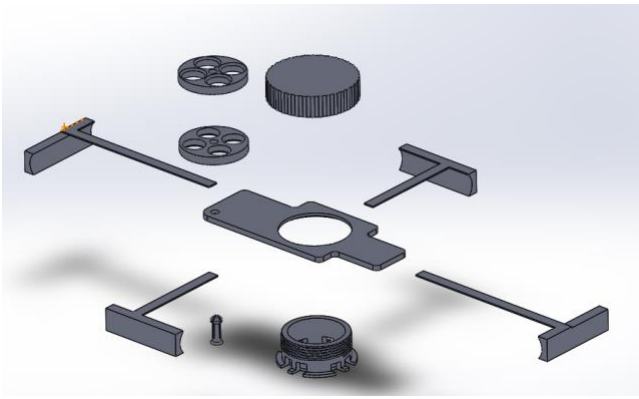


Figure 33: Exploded and Assembled View of Spectrographic Analysis Tool

This tool was assembled from 3D printed parts. Each component was printed from polylactic acid (PLA) filament on the Additive Manufacturing lab's 3D printers. This iteration of the tool is different from the initial design to compensate for printing errors in the previous design.

Four clamps positioned radially from the screw cap hold the tool in place on the driver's phone, while the screw cap keeps the clamps fixed. The dial in the top corner contains the three filters for the photographs.

Figure 34 below show the completed spectrographic analysis tool both disassembled and assembled.

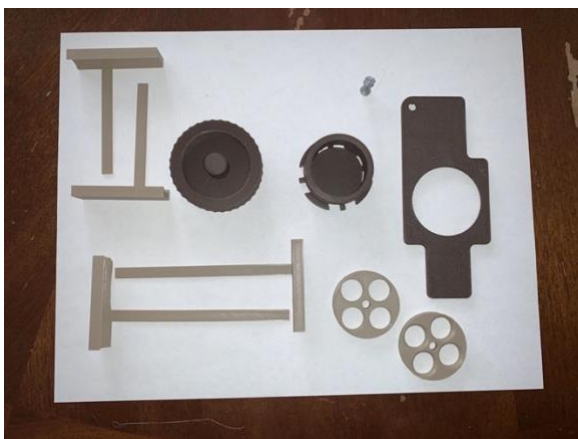


Figure 34: Disassembled tool(left), assembled tool(right)

Figure 35 shown below are the four pictures taken with the spectrographic analysis tool.



Figure 35: Pictures of Spectrographic Analysis

The instrument deployment task requires the team to deploy a solar powered light in a specific orientation along the course. This tool is composed of a solar panel wired with an LED, a resistor and switch, inside of a case with an externally mounted compass. This case was then mounted on a tripod for ease of deployment. *Figure 36* shows the completed instrument deployment tool.



Figure 36: Instrument Deployment

As seen above, the LED was not as bright as would be ideal. Future teams will need to test multiple resistors to find the optimum size for ease of use.

The core soil sample retrieval task can be completed by the tool shown in *Figure 37* below.



Figure 37: Soil Sample Retrieval Tool

This tool can be used to retrieve samples with an approximate volume of 50 mL based on tests conducted. This volume is approximately three times the minimum required for competition. The previous design with the step lever as a handle was abandoned due to the ease of manufacturing and structural integrity of this tool.

The solid and liquid sample retrieval tasks can be accomplished by the same tool. The tool will need to remove material from a receptacle five and a half inches in diameter and three inches deep. The tool must also be sanitized between uses. *Figure 38* below shows the current state of the design for this tool.

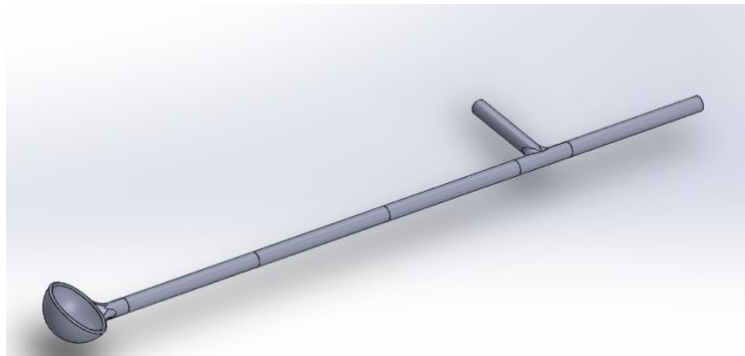


Figure 38: Solid and Liquid Sample Retrieval Tool

This tool is designed to collapse into four rods, a scoop and a connection piece handle, The pieces can then be stored on the chassis of the rover out of the way of the drivers. The tool is approximately four feet long and the team is waiting to get the pieces back from the 3D printing lab.

Galileo Wheels

Design

The Galileo Rover wheel sub-team seeks to keep the current design from the Denver Endeavour team. This will allow us to stay within the goal of minimizing the weight of the rover,

by maintaining each wheel at a maximum of 10 pounds. The current diameter of each wheel at 27in will remain the same as the outer wheel carcasses have already been made out of multiple layers of carbon fiber. This redesign from the previous team will remain due to their intention of strengthening the carcasses' geometry, and will help prevent deformation during competition. The Odyssey team decided to add u-type channels to reinforce the additional stress on each wheel during competition, particularly in turning and climbing. The wheel sub-team determined these supports will not be necessary for the Galileo Rover, although proper testing needs to be completed to confirm this assumption.

The polyurethane foam has a thickness of 1in and will be bonded together, then those layers will be bonded to the wheel carcasses. The overall wheel design will remain from last year's design, as well as the outer tread layers made of polyurethane rubber at 27 in. The assembly of the full wheel is shown below in *Figure 39* with an exploded view shown in *Figure 40*.

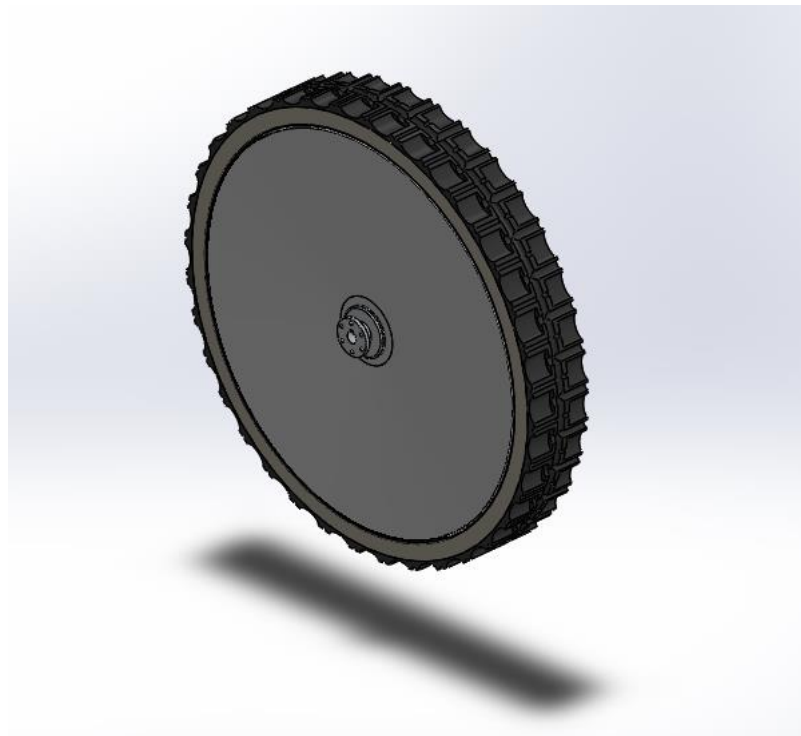


Figure 39: Full Solidworks Rendering of Wheel Assembly

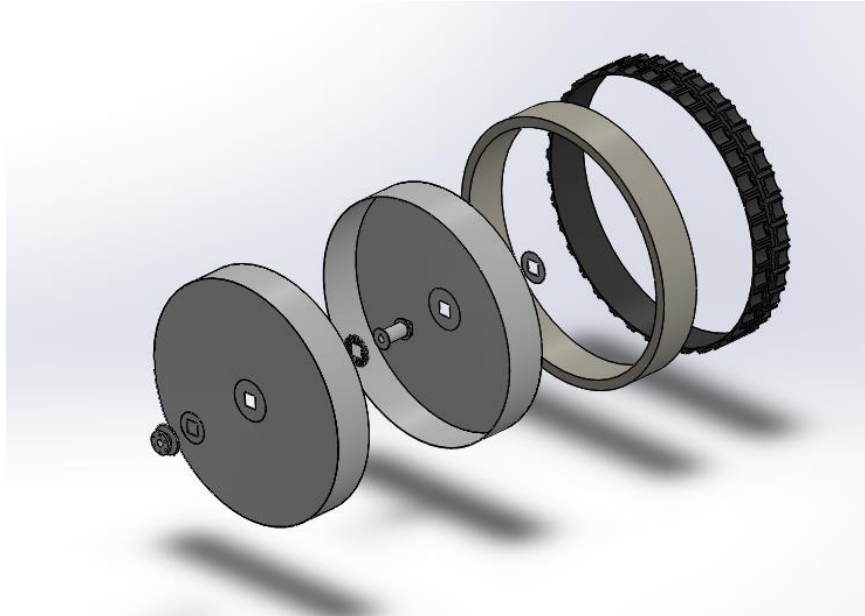


Figure 40: Exploded Solidworks Rendering of Wheel Assembly

Hub Assembly

The hub assembly design will remain as is from the Denver Endeavour wheel sub-team. In order to determine their design will be sufficient, we conducted a finite element analysis on the hub itself as shown below in *Figure 41*. For the hub assembly analysis, a moment around each plate was used with locking the brake rotor mount to act as if the rover is travelling at full speed and coming to a complete stop, causing a moment around the axle. Using a moment on all four hub mounts was decided on, due to the fact that these plates are going to be glued to the carbon fiber dishes using Loctite 9309. A mold will be created to keep the hub and the carbon fiber as centric as possible while the epoxy cures.

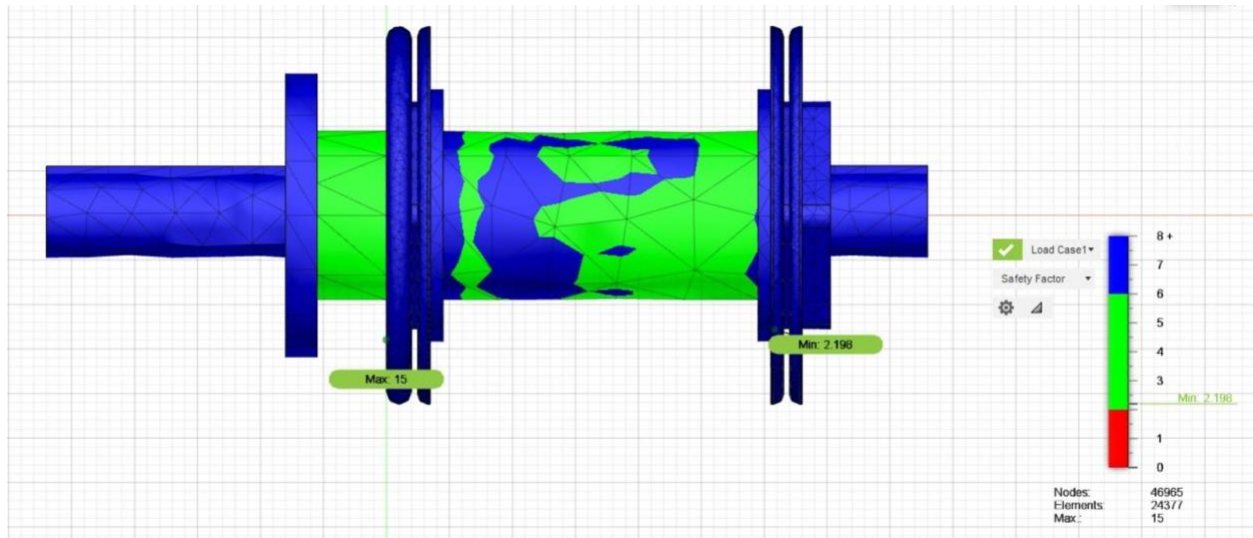


Figure 41: Finite Element Analysis Rendering in Fusion 360 on Hub Shaft Assembly

The fully updated wheel assembly as shown in *Figure 42* is the current design of the hub shaft components as designed by the previous rover team, Denver Endeavour. This design will remain, with the reduction of the center portion by 1in and the reinforcement disks going from 4 to 3inches in diameter. Each of these improvements made by Endeavour will help in reducing the maximum weight in each wheel by 5 pounds, resulting in an overall weight reduction of 15 pounds for the whole rover. Due to the orientation of the wheel carcasses being opposite of each other, the bolt side of the hub shaft will be placed inside the brake side carcass. Each carcass has reinforcement disks that will adhere to the inner and outer portions of the wheel carcass when the full assembly is completed, as shown in *Figure 43*.

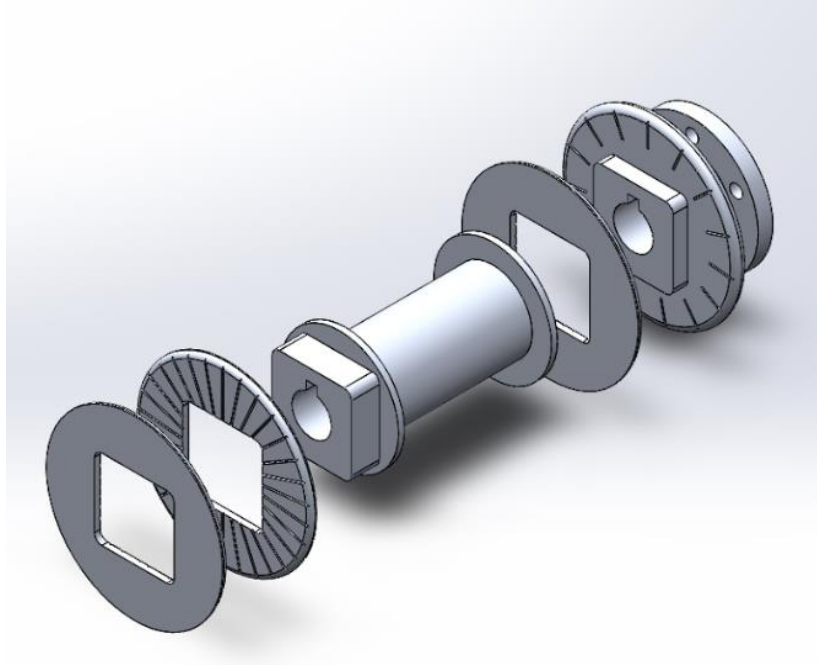


Figure 42: Exploded View of Wheel Hub Assembly

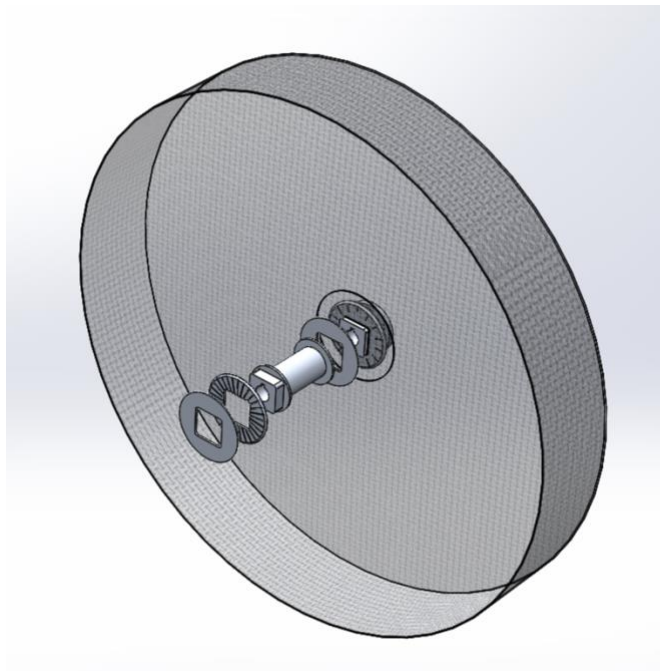


Figure 43: Wheel Hub Shaft Components with one Wheel Carcass

The previous Odyssey Rover team decided to add u-type channels in the rear wheel in order to prevent stress deformation when turning and traversing over inclines. It was confirmed

by the Endeavour team that this will not be necessary with the new wheel geometry and the orientation in which the layups were completed. The Odyssey team decided to go with 7 different concentric layers during their carbon fiber layups: 10in, 12in, 14in, 22in, 23in, 24in, and 26in. With the new design by Endeavour being 5 layers: 8in, 14in, 22in, 24in, and 26 in, along with a 0, 45, 90, 45, 0 degree layup orientation, this will eliminate the need for u-type channels.

Testing

In order to move the analysis and testing process along, the riders for the Galileo Rover team were pre-selected and their weights were used to complete the analysis on the wheel and wheel hub. The two riders are Hannah and Kilian, with a combined weight of 360 lbs. The Endeavor's team m-file shown in *Appendix C*, was modified accordingly to account for the Galileo Rover's vehicle weight in order to get a new maximum braking force on the rear wheel. This braking force is applied as a torsion between the axle and hub assembly. The value was determined to be 308.2291ft-lbs and was rounded to 325ft-lbs in order to complete the finite element analysis using Fusion 360. With this force applied, the analysis yielded a minimum safety factor of 2.2, and therefore the wheel sub-team decided to keep the current hub shaft design. Due to the limitations of finite element analysis in Solidworks with a material such as carbon fiber, the wheel team is planning on seeking an alternate route for completing the carbon fiber analysis. The previous Endeavour team had attempted doing an analysis in Abacus but had issues with importing a Solidworks file into Abacus and therefore were unable to successfully complete this. The stress concentration of the carbon fiber is extremely important and will ultimately determine whether the wheel will be able to withstand the forces being applied. In order to determine the alternate stresses acting on the wheel, the wheel sub-team modified the

existing m-files in *Appendix C-F* to match the current Galileo Rover weight, but kept the sidewall angles the same as previously determined by Endeavour. With a minimum safety factor of 2, the sidewall thickness for the Galileo wheels was 0.3719 inches compared to a minimum of 0.3714 inches required for the vertical sidewall. The hoop stress m-file as shown in *Appendix D*, gives Galileo's minimum wheel hoop thickness to be 0.004642 inches. Therefore, the bending moment at the hub was recalculated accordingly with Galileo's changes, and was determined to have a safety factor of 95.

Manufacturing

The manufacturing process in which Galileo Rover used was adopted from the Odyssey team. The same 3D printed tread mold, MDF, and breaker board was used to properly pour the polyurethane rubber mixture. The polyurethane mixture is equal parts, A and B, and once mixed for 2 minutes, can be poured into the mold, as shown in *Figure 44*. The mixture must be mixed thoroughly to ensure no bubble would form and therefore cause issues when the rubber cures. This was first completed by making sure the mold had no possible leakage points to where the rubber could potentially pour out as it expands and cures. In order to ensure this, the mold was sealed with clay, showing yellow mold surrounding the tread mold. The team decided to apply Vaseline to the inside of the tread mold and outer side of the breaker board where the rubber will come in contact, in order to prevent the rubber from getting stuck inside the mold and allow for an easier removal process when the mold has cured. Once this was completed, the process began by each team member measuring their pour, stirring parts A and B together, and eventually pouring into the mold. The polyurethane was poured in two sections, as recommended by Kevin Fornall. This would allow the rubber to naturally flow around the mold as each pour is made and prevent an uneven rubber tread when cured. Once the liquid polyurethane met the same height as

the tire tread, tongue depressors were used to slowly drag the mixture around the mold in order to ensure it was even. Another suggestion the team took from Kevin was to make sure the liquid was just over the top of the tire tread mold, that way when it cures it will not be uneven. After 48 hours the team returned to the first mold pour and determined the polyurethane did not cure correctly, as there were parts that were not dry and the color was not the same throughout. Once adjustments were made, the team continued with the same process and made sure the mixtures were properly stirred before pouring. This turned out to be successful, as each of the 4 treads cured correctly, as shown in *Figure 45*, and were completed.



Figure 44: Pouring Polyurethane Rubber



Figure 45: Complete Rubber Tread

The next step for the Galileo wheel sub-team was to create a fixture to ensure the hubs will be hub centric when epoxying them to the carbon fiber wheel carcasses. The team decided to make a 2-in-1 fixture allowing for the hubs to be hub centric as well as to account for pouring the foam layer. The idea is that the hubs can be epoxied as centric as possible in relation to the carbon fiber. In order to design this fixture SolidWorks was used to design it. First, the team found a piece of medium density fiber, MDF, board in the shop, and decided this would be sufficient for the fixture. The measurements of the MDF, thickness of tire tread, hub diameter, diameter of the carbon fiber carcasses and the inner diameter of the foam breaker board which will serve as the outermost piece were taken. The team decided to adopt the same design as the rubber tread mold that Odyssey created. Once this was completed, a model was drawn in Solidworks, as shown in Figure 44. The thickness of the tire tread was needed in order to make sure there was proper room between the two breaker boards to fit the tire tread and also pour the foam. The depth of cut for the inner and outer diameters was determined to be $\frac{3}{8}$ " as this is about half of the total MDF thickness of 0.754", and will be sufficient for the breaker board to sit into.

This drawing, as shown in *Figure 46* was transferred to Fusion 360 to begin the machining process.

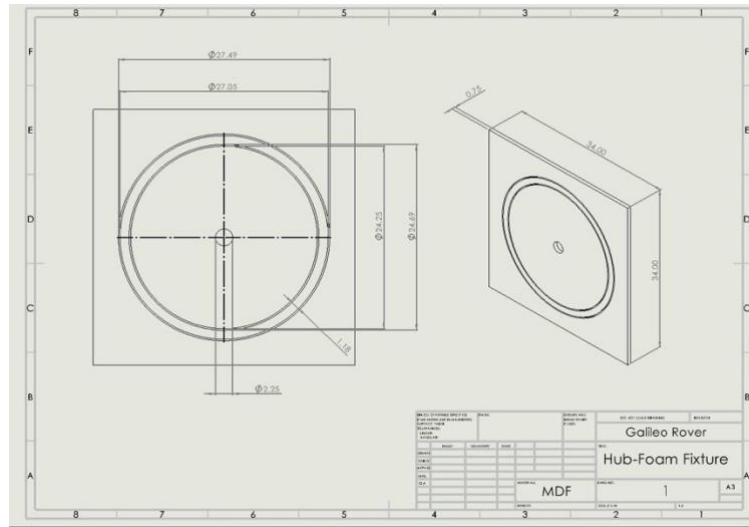


Figure 46: Solidworks Drawing of Hub-Foam Fixture

With the help of Professor Doug Gallagher, the Shopbot tooling was chosen. The team decided to use a 3/16" ball end mill for the inner and outer diameters and a 1/2" ball end mill for the smaller circle that will be cut through where the hub shaft will be placed. Despite having somewhat of a learning curve with the Shopbot and how it functions, the Fusion program was created and successfully run on the Shopbot, as shown in *Figure 47*.

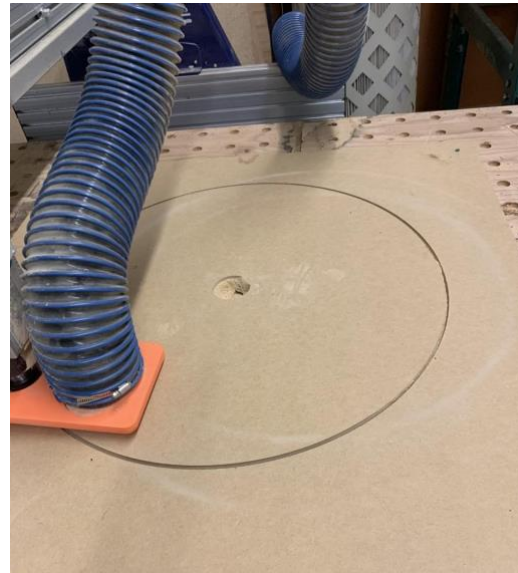


Figure 47: Shopbot Tool Path of Fixture

Manufacturing of Spokes

After completion of the wheel assembly and further analysis of the carbon fiber surrounding the hub shaft, there was notice of possible oil canning taking place. This could create failure at the hub due to the lateral forces on the wheels under loading, and could potentially compromise the integrity of the wheels. Possible solutions consisted of u-type channels as previous teams have used, but due to our wheels already being assembled this was no longer an option. The next choice was to go with aluminum spokes on the outside of the wheel. These would extend from the hub shaft to the outer portion of the wheel with four on each side, making eight total for each wheel. Each spoke has a length of 10 inches, with 2 holes drilled at a ½” diameter, as shown in the Solidworks rendering in *Figure 49* below. This part was designed in Solidworks and moved to Fusion 360 for manufacturing.

The decision on whether to adhere the aluminum spokes with epoxy or screws/bolts is to be determined further by FEA analysis. When running the FEA analysis on the wheels, the draft angle in the carbon fiber carcass made this extremely difficult to mate the spokes to the carbon fiber. Therefore, further analysis on the aluminum spokes must take place due to previous unsuccessful attempts on FEA in Solidworks. After consideration, we decided to go with shoulder screws to combine the aluminum to the carbon fiber to fasten the spokes onto the wheel. The shoulder screw chosen is a 3 ¼” and ½” diameter screw.

To optimize the manufacturing, 8 spokes were stacked on top of each other and machined simultaneously. The dimension of the part was altered in Fusion to match the thickness of 8 spokes laying on top of each other. The part was then uploaded to Fusion to run the G-code for the machine to manufacture the part. The manufacturing feature in Fusion allows for the user to

upload a part file and enter the machine tools and the order they are in the machine. To start, open your part file and configure the size of stock that will be manufactured, as shown in *Figure 48*. Then create a tool path using the 1/2" flat end mill. After the tool path is confirmed, the G-code file can be created to send to the CNC mill. The body of the spokes were machined using the Haas T2 CNC mill. To begin, the stock must be secured down to the machine's worktable. Next, the machine must be programmed to find its center. To do this, we had to define our zero using the probe tool for the z axis and centering the machine on top of the stock we used to set the X and Y axis. Then the file from Fusion is sent to the mill after the coding is created. Once the file is uploaded to the machine, the correct file must be chosen to let the machine know what tool and path to use. After the correct tool path is chosen, the doors of the machine must be properly secure and closed before the machine will start. After machining all 32 spokes the next step will be to drill the 1/2" diameter holes in order to adhere the spokes to the carbon fiber as well as drill the holes in the carbon fiber for the shoulder screws. After adhering the spokes the final step will be to pour the foam layer between the carbon fiber and the rubber tread layer. A final assembly of the wheels is shown in *Figure 50* below.

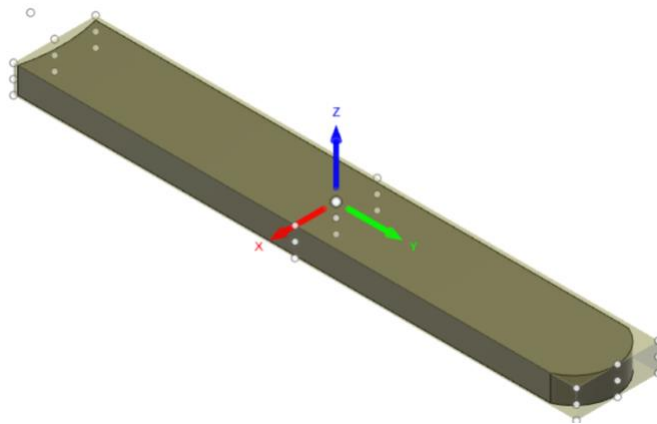


Figure 48: Fusion 360 Stock Orientation

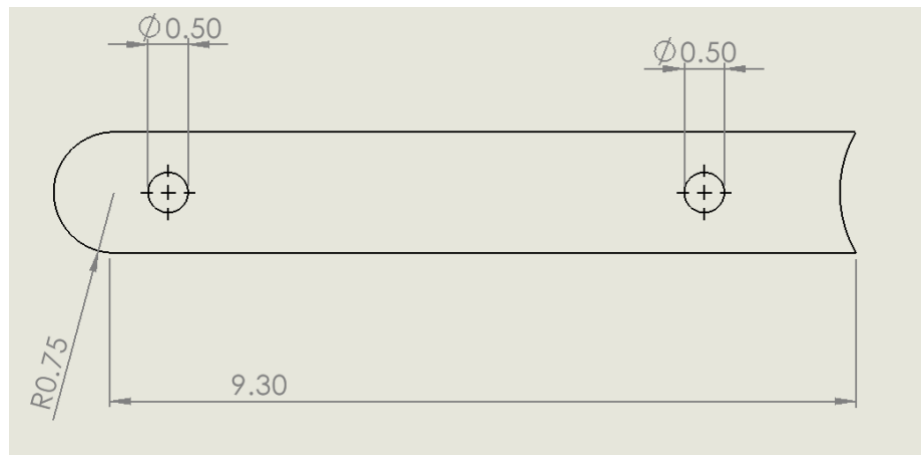


Figure 49: Dimensions of Wheel Spoke

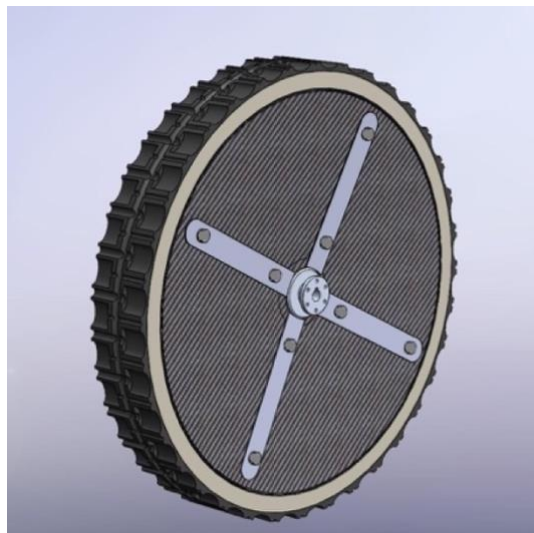


Figure 50: Solidworks Rendering of Final Wheel Assembly with Aluminum Spokes

Wheel Assembly

The assembly of the carbon fiber wheels consisted of the following materials; carbon fiber carcasses, wheel hub and disc components, acetone, scotch brite pads, and EA 9309 epoxy mixture. Each wheel consists of an inner and outer shell component, one hub shaft and three hub-to-wheel reinforcement discs. The carcasses are composed of multiple layers of carbon fiber in which will nestle inside one another. In order to properly assemble the wheels together, the hub

shaft components and inner/outer carcass were done almost simultaneously. A series of steps were completed to accomplish this task.

After consultation with Kevin Fornall, it was suggested that first, holes are to be drilled into the outer shell of the carbon fiber carcass approximately 10 inches apart. This was recommended to allow us to drill slits 1 inch from the bottom of the carcass up to the top, in order to have the end goal of combining the carcass shells in the easiest way possible. The slits were drilled using a hand saw at the approximate hole location. Water was also added while drilling in order to reduce carbon fiber particles from spreading. Once this was complete, the wheel team used scotch brite pads and acetone to sand and clean the carbon fiber shells where the epoxy will be applied. The acetone was also used to clean the aluminum hub shafts and hub centric disks. The fixture created last semester was utilized to ensure the wheel would remain hub centric and to allow for proper assembly as shown in *Figure 51*. The axle was utilized in the hub shaft to allow for stability, and was taped to prevent from possible epoxy spills.



Figure 51: Image of Carbon Fiber on MDF Fixture

Once all of the required pieces were cleaned, the EA9309 epoxy was mixed together. This mixture comes in two parts, A and B, with a 100 to 23 ratio, respectively. Once combined

fully for 3 minutes, the mixture is ready for use. The outer portion of the hub shaft assembly was added to the small hole in the MDF fixture. This piece can be seen in *Figure 47* above, on the left. The epoxy was then applied to the hub centric disk in order to combine it with the piece currently in the fixture. Then, the outside of the wheel carcass was applied with epoxy, as well as the opposite side of the disk that will come in contact with the carbon fiber. Once this took place the rest of the hub shaft assembly was put together as shown above in *Figure 42* and *Figure 43*, applying epoxy to the respective sides. Once the hub shaft was adhered to the inside of the outer carcass, the last disk was applied to the outer, inner carcass to properly combine one wheel together shown below in *Figure 52*. The goal was to have the outer most disk sit in the square side of the hub shaft. This wasn't the case with each wheel, and applied human force to the top wasn't enough. Additional aluminum pieces and table clamps were added to provide weight and constant pressure to the top of the wheel in order to secure the wheel together.

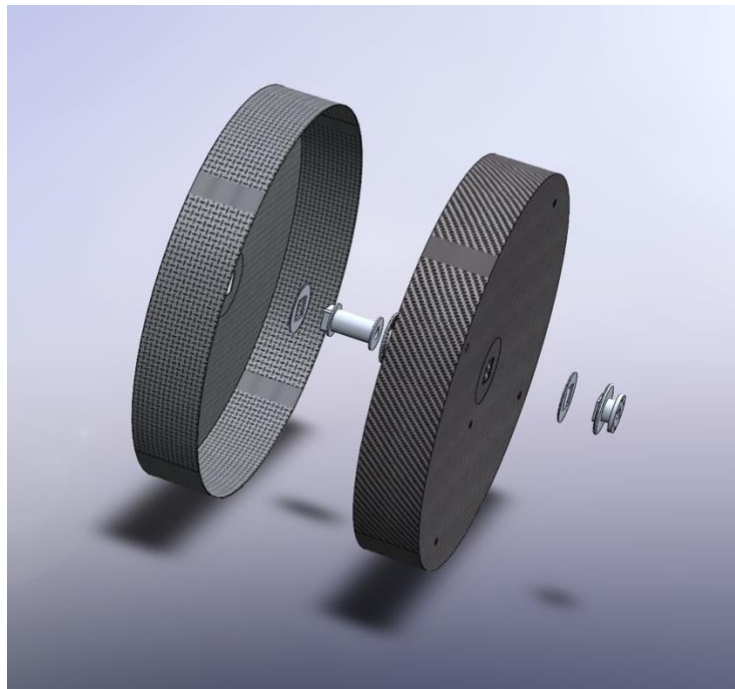


Figure 52: Exploded Solidworks Rendering of Wheel Assembly

After the completion of the carbon fiber carcasses and hub shaft assembly, the outer carcass and inner carcass combination took place. The epoxy was applied in between the two carcasses using a tongue depressor. The goal was to get as much epoxy as possible inside these two pieces and to spread consistently around the diameter of the wheel. Once this was completed, a hose clamp was adjusted to secure the two carcasses together. This hose clamp was secured extremely tight around the outside of the wheel, as shown in *Figure 29* above. The idea was that this added pressure would allow the carbon fiber carcasses to adhere to one another while the inner hub shaft was bonding. The wheel assembly was let cure for 3-5 days. The result of this procedure proved to be successful. Each component was properly adhered to each other with no areas of concern.

Wheel Foam Pour

In order to properly prepare for the foam pour, a few areas of concern were addressed before set up took place. First, the team needed to make sure the fixture manufactured above was suitable and can withstand the expansion of the foam as it begins to cure. It was determined that a new outer diameter was needed in order to allow the foam outer piece to 'sit' in the fixture properly to prevent leakage of liquid foam. This outer diameter was created using the Shopbot and a 1/2" endmill that increased the overall outer diameter to 27.75", as shown below in *Figure 53*, outlined in blue. Once this was completed, the foam outer mold sat flush in the fixture.

After the fixture was altered in order to prepare for an accurate foam pour, the team began with set up. First, acetone was used to clean off all sides of the carbon fiber as well as clean up the inside of the tread, in order to prevent the foam from not adhering to the rubber properly. Then, plastic wrap was laid across the fixture making sure all parts were covered. This

wrap would help prevent the foam from leaking under the outer ring and essentially lifting the tread and carbon fiber as it expands as well as sticking to the MDF fixture. Next, the team laid the carbon fiber wheel hub in the inner most portion of the fixture to ensure the wheel was as flat as possible. Once this was completed the tread was inserted into the outer foam MDF breaker board to keep the tread as circular as possible around the carbon fiber when the foam is poured. This piece was secured into the fixture's outer diameter with a snug fit. The top of the carbon fiber was taped to account for the expansion of the foam. Once this was done, the team was ready to pour the foam.

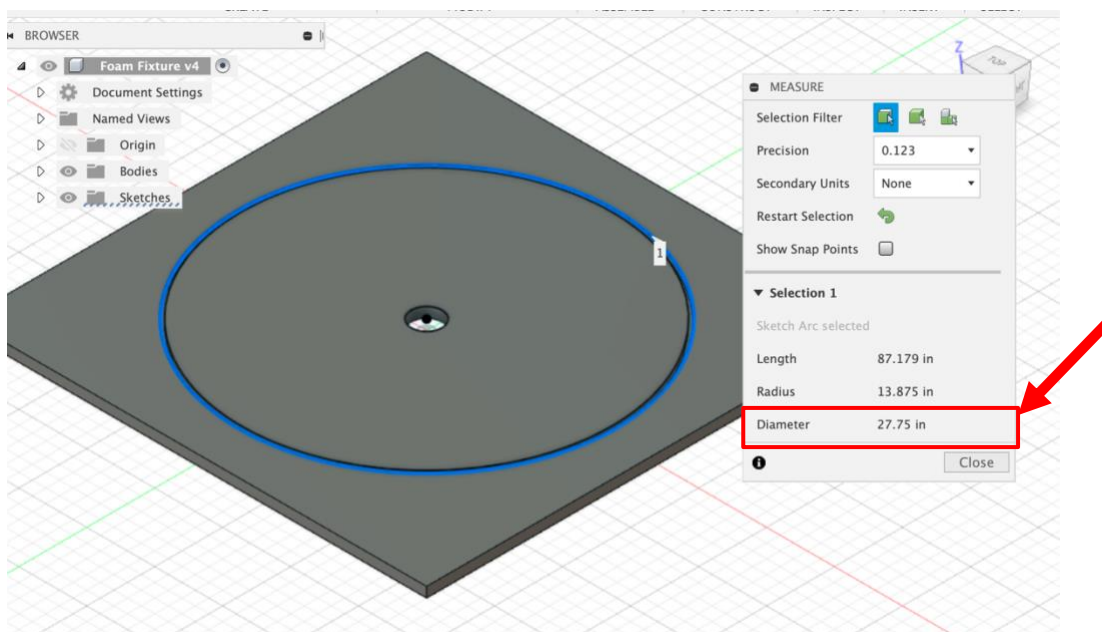


Figure 53: Fusion 360 Rendering of New Outer Foam Diameter

The foam mixture Galileo used was FlexFoam-iT! 25 and a detailed data sheet can be seen in Appendix G. This particular mixture has the highest density foam and expands the least and was also used due to the left over material from previous years, although the team did purchase more this year. The mixture consists of two parts, A and B, with a 1 to 2 ratio. Both parts A and B liquid are combined, mixed and poured. Once poured, as the liquid begins to cure

it creates a solid, flexible foam. The team started with pouring part A to 192g, and part B to 384g. Once this was completed, part A was combined with part B and mixing began with a stir stick. After these were fully mixed, the liquid pour took place and was aimed directly between the tread and outer portion of the carbon fiber. As the foam began to expand the team watched carefully in order to determine how much more liquid foam was needed. Once evenly spread around the wheel, the foam was let cure for 2-3 days. Weight was added to the top of the carbon fiber and outer MDF ring in order to prevent the expanding foam from lifting out of the fixture, as shown below in *Figure 54*. These weights were then secured using table clamps. After the foam was fully cured, the team began disassembling the fixture and clamps as well as removing the outer foam ring to get the completed wheel out. Once this was completed, the foam was cleaned up around the carbon fiber, and a final product of the wheel assembly can be seen in *Figure 55* below.



Figure 54: Wheel Pour Set Up



Figure 55: Final Assembly of Wheel

Areas for Improvement

While assembling the wheels, Galileo noticed areas that could use some improvement in the design and manufacture phase. The draft angle at which the inner and outer carbon fiber carcasses combine could be altered in order to prevent the oil canning that was experienced at the hub of the wheel. This would also eliminate the need for aluminum spokes on the outside of the wheel. Instead, inner u-type channels can be utilized to prevent this and also add a better overall appearance of the wheels. Galileo was pressed for time and need a solution as soon as possible, therefore the team decided to add outer wheel spokes bolted on to the carbon fiber. This addition proved to strengthen the wheels at the hub and prevented possible failure. The team also noticed that improvements to the foam fixture would be beneficial to prevent the leakage of foam from getting under the bottom side of the wheel. A custom fixture that could potentially account for the tread thickness and diameter could be a solution, instead of relying on the foam ring to secure properly into the MDF fixture. This also leads into the rubber tread not being consistent all the way around, meaning the thickness of the tread is not maintained throughout all portions of the wheel. This prevented the team from creating a more secure option on the fixture. Due to this inconsistency, there wasn't a way to account for this and create a ring using the Shopbot for the tread to sit into. If this were the case, the wheel would have had a more accurate foam pour, as

the wheel would sit more centrally and the same distance between the carbon fiber outer shell and tread would be consistent all the way around. Lastly, the team noticed the hub shafts were adhered unevenly therefore, preventing the axel to slide all the way through using the keyway. In order to fix this issue, the team used the Vectrax mill and a 11/16mm reamer to re-drill the inner diameter holes in the hub shaft to account for the axel diameter and allow the axel to properly fit in the hub. This can be seen in *Figure 56*, below. Once this was completed, the axels fit with proper clearance all the way around and allowed the wheels to be successfully mounted to the frame of the rover.

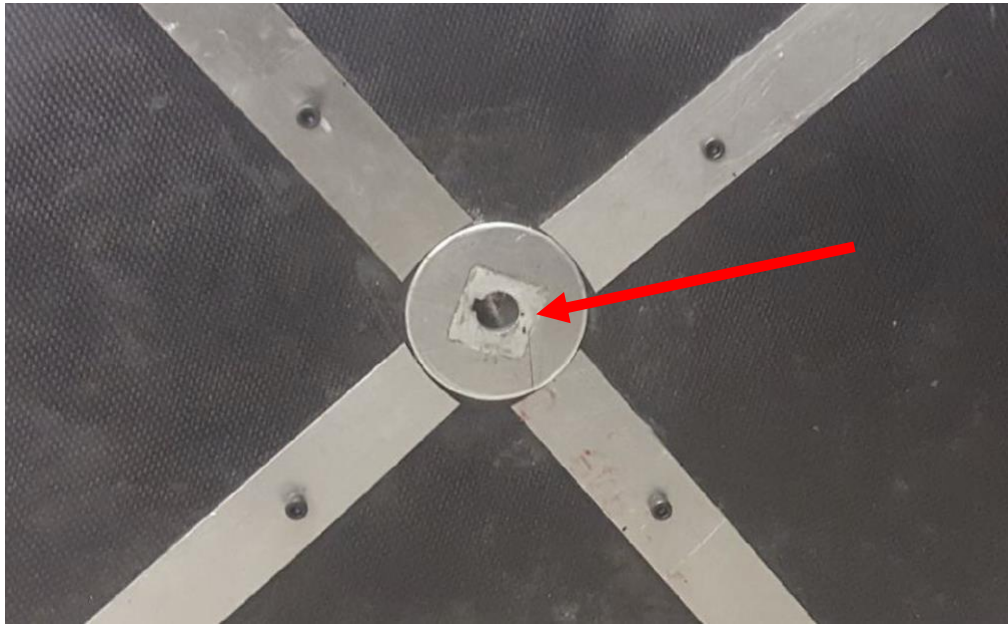
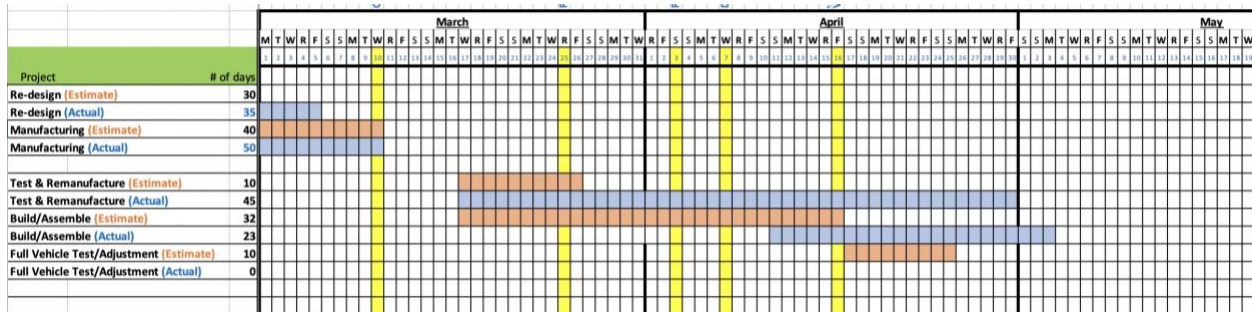
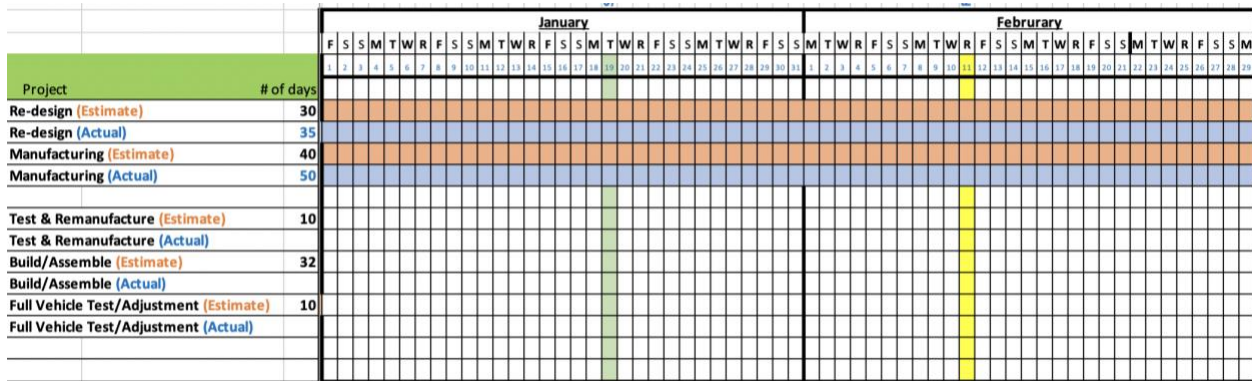
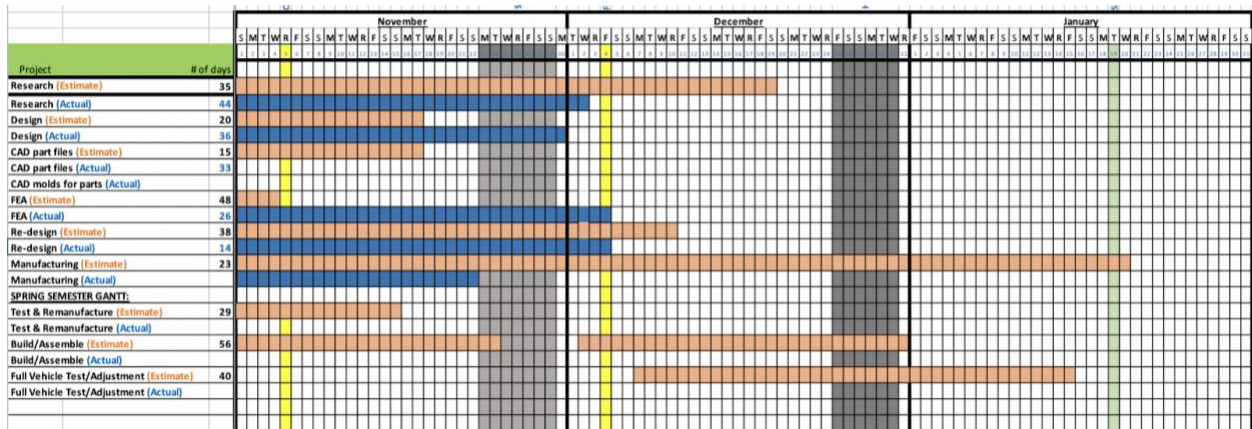
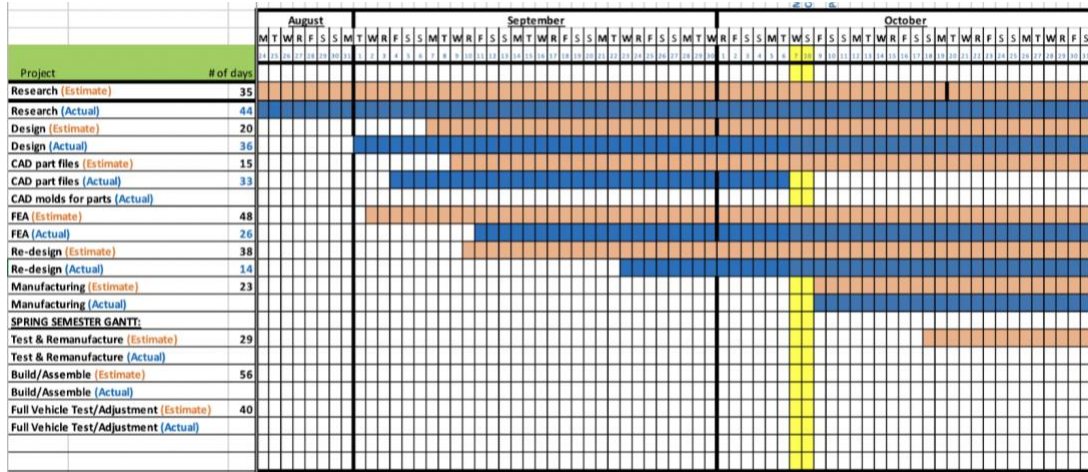


Figure 56: Inner Diameter of Hub Shaft Re-drilled to allow axel to fit through

Budget/Costs

Galileo Rover's budget mainly consists of travel and purchase of miscellaneous items such as, bolts, nuts, paint, gloves, etc. The total estimated cost is \$7,250.00, with travel being the majority of the cost. The Galileo team plans to travel 2700 miles from Denver, Colorado to Huntsville, Alabama via a rental van. Similar to Endeavour's analysis, we have accounted for food and lodging for 7 people and by utilizing a van large enough to accommodate the whole team, this will provide some cost savings as well. The plan is to share hotel rooms along the way and at competition in order to keep costs down for lodging, therefore an average room rate for the time of year was used. Galileo may need to purchase more items throughout the semester, but that is yet to be determined until the assembly of the wheels, frame, etc. takes place. A breakdown of Galileo Rover's estimated budget is shown in *Appendix A*. An updated budget, not accounting for travel due to a virtual competition, can be seen in *Appendix B*.

Gantt Diagrams



References

Odyssey Rover Team 2017-2018

Denver Endeavour Rover Team 2018-2019

Professor Doug Gallagher

Previous Team Lead Madison Gast

Machine Shop Expert Nicholas Diamond

Composites Expert Kevin Fornall

Machine Shop Expert Jac Corless

National Aeronautics and Space Administration (2020) *2021 Rover Challenge Guidebook*.

Science Learning Hub. (2011, February 22). *Pedal power*.

Kumar, A. (2020, September 22). *Hafthor Bjornsson breaks world record with 1,104-pound deadlift*. ESPN.

Appendices

Appendix A: Estimated Budget

Component	Material	Cost
Wheels	Carbon Fiber Roll	~ \$300
Miscellaneous	Bolts, nuts, hinges, paint, gloves, epoxies	~\$250 for misc. items

Travel	Quantity	Cost	Total Cost
Hotel	8 nights, 3 rooms	\$130/night	\$ 3,120.00
Rental Van	1 van, 8 days	\$200/day	\$ 1,600.00
Gas	2700 miles, 15mpg	\$2.70/gal	\$ 486.00
Food	7 people, 2x/day	\$10/meal	\$ 1,400.00
		Total	\$ 6,606.00

Appendix B: Updated Budget

Items Purchased	Total Cost	Updated Balance
Starting Balance	\$1,800.00	\$1,800.00
Klean-Strip 1 qt. Acetone	\$25.76	\$1,774.24
H287S MGS Hardener QT SLOW	\$154.83	\$1,619.41
4130 Alloy Steel Round Tube	\$34.81	\$1,584.60
Fasteners	\$209.96	\$1,374.64
FlexFoam	\$210.69	\$1,163.95
Shock Pump	\$35.00	\$1,128.95

Appendix C: Breaking at Hub

```
W = 520; % Weight of Rover + Riders in lb
L = 85; % Length of Wheelbase in inches
l1 = 40; % Distance to CG from front wheels in. inches
r_r = 85; % Rotor radius in mm
r_w = 13.75; % Wheel radius in inches
angle = 30; % angle of ramp in deg
h = 10; % height of CG from ground in inches
mu = 1; % Coefficient of Static Friction between road and tire surfaces
%% Calculations
l2 = L-l1; % distance from rear wheel to CG
angle = angle*pi/180; % convert angle to radians
r_r = r_r/(25.4*12); % convert rotor radius to feet
r_w = r_w/12; % convert wheel radius to feet
Fn_f = (W*cos(angle)*l2+W*sin(angle)*h)/L; % Normal Forces on Front Wheels Combined
Fn_each_f = Fn_f/2; % Normal Force on each front wheel
Fn_r = W*cos(angle)-Fn_f; % Normal Force on rear wheel
sumF_n = Fn_f+Fn_r; % Total Normal Force on all wheels
Fb_max_f = 2*mu*Fn_f; % Maximum Braking force that could be applied to front wheels
Fb_max_f_each = Fb_max_f/2; % " " to each front wheel
Fb_max_r = mu*Fn_r; % Maximum Braking force to rear wheel
T_front = Fb_max_f_each*r_w % Torque on each front wheel
T_rear = Fb_max_r*r_w % Torque on rear wheel
Fb_min = W*sin(angle)
```

Appendix D: Hoop Stress

% Hoop Stress- Galileo

% Calculates minimum circumferential surface thickness assuming:

% 520lb load, only one tire in contact with the ground

% 27" diameter * 4" thickness

% Models wheel like thin walled pressure vessel

% For thin wall assumptions to be valid the diameter/thickness > 20 must be
% the case.

%

% 7000psi UTS for CFRP

load = 520; % pounds

D = 27; % inches - wheel diameter

w = 4; % inches - wheel thickness

UTS = 7000; % lowest value for CFRP UTS found on MATWEB

Pressure = load / (D*w);

t = (Pressure *D) / (4*UTS)

Appendix E: Sidewall Thickness

% Sidewall Thickness Required

% Solves required sidewall thickness

% Assumptions:

% The load of the vehicle, transmitted to the wheel through the wheel hub is supported by CFRP in tension only. Integrating thickness*sin(O) from 0 to pi,

% this means the cross sectional area of CFRP supporting the load is 2*thickness.

% Research gives UTS values for CFRP 487 - 825MPa, but yield strength

% ranging from 945 - 1080 Mpa. Using the lowest value available, 487MPa

% roughly equals 7000psi

% If stress = force over area, area = force over stress. Area equals 2t.

% $t = \text{Force} / (2 * \text{stress})$. Although there are two sidewalls, we'll use a

% safety factor of two, and NOT make the equation $t = F / (4 \text{ stress})$

% Assume vehicle weight is 520 pounds, and only one wheel is in contact with

% the ground

P = 520; % pounds

Stress = 7000; % psi

$t = P / (2 * \text{Stress})$

% Above was for a vertical sidewall

% Since Endeavour sidewall is at a slight angle we must use trig to calculate the

% forces in the sidewall

dx = .5; % length of the inset of the angled bit

dy1 = 9.9; % height of the angled bit

dy2 = 9.78; % height of the slightly shorter side angled bit

theta1 = atan (dx/dy1);

theta1d = theta1*180/pi % angle of endeavour sidewall degrees

theta2 = atan (dx/dy2);

theta2d = (180/pi)* theta2 % angle of endeavour sidewall degrees

p_1 = P/cos(theta1) % force along the hypotenuse

p_2 = P/cos(theta2) % force along the hypotenuse on the other side

format long;

t1 = p_1/(2*Stress)

t2 = p_2/(2*Stress)

Appendix F: Bending at Hub

% Bending at Hub - Galileo Rover

```
v = 15;      % enter speed in mph
W = 520;    % weight of vehicle and drivers lbf
r = 17;     % turning radius
Sy = 213000; % Tensile strength of material in psi
n = 2;     % safety factor
v = v*5280/3600;% puts speed into ft/s
m = W/32.2; % converts weight in pounds into mass in slugs
a = v^2 / r; % radial acceleration
F = m*a     % sideward force exerted in the tire
t = .048;
b = 12.4;
w = 4;
I = (1/12)*b*w^3 - (1/12)*(b-2*t)*(w-2*t)^3; %moment of inertia
M = F*b
sigma = (M*(w/2))/I;
SF = Sy/sigma
```

Appendix G: Flex Foam Data Sheet

FlexFoam-iT!™ Series

Flexible Polyurethane Foams

3lb., 4 lb., 5lb., 6 lb., 7 lb., 8 lb., 10 lb., 14 lb., 15 lb., 17 lb., 23 lb. or 25 lb.



www.smooth-on.com

PRODUCT OVERVIEW

FlexFoam-iT!™ Series foams are premium quality water blown flexible foams that can be used for a variety of industrial, special effects and art & crafts and projects. With several to choose from, uses include making theatrical props (swords, knives, hammers, etc.), industrial gaskets, custom padding and cushioning, and more. FlexFoam-iT!™ foams are also used as repair materials for seats, cushions and archery targets. SO-Strong™ colorants can be added for color effects.

Part A and B liquids are combined, mixed and poured into a mold or other form (apply release agent if necessary). Mixture will rise and cure quickly to a solid, flexible foam. Foams vary by density and offer good physical properties. The lower the number, the more the foam expands. **FlexFoam-iT!™ III** is the lowest density foam and expands the most. **FlexFoam-iT!™ 25** is the highest density foam and expands the least. **FlexFoam-iT!™ 15** has a relatively long, **2 minute pot life**.

- **FlexFoam-iT!™ IV** and **FlexFoam-iT!™ 15** are "Tuff Stuff" foams which are exceptionally strong.
- **FlexFoam-iT!™ 6** and **FlexFoam-iT!™ 8** are "Pillow Soft" foams with a similar softness to pillow or cushion foam.
- **FlexFoam-iT!™ 7 FR** is **Flame Rated** to **FMVSS-302** specification
- **FlexFoam-iT!™ 23 FR** is **Flame Rated** to **UL-94 HB** specification

8oz./237ml. of FlexFoam-iT!™ A+B
poured into a 32oz./946ml. cup.



TECHNICAL OVERVIEW

	A:B Mix Ratio by Volume	A:B Mix Ratio by Weight	Specific Gravity (g/cc) (ASTM D-1475)	Specific Volume (cu. in./lb.)	Pot Life (Cream Time) (ASTM D-2471)	Handling Time	Cure Time	Approximate Volumetric Expansion	Approximate Lbs. / Cu. Foot = Kgs. / Cu. Meter
FlexFoam-iT!™ III	1:2 pbv	57.5:100 pbw	0.05	504	35 sec.	25 min.	2 hrs	15 times	3 lb/ft ³ = 48 kg/m ³
FlexFoam-iT!™ IV	N/A	80:100 pbw	0.06	420	30 sec.	45 min.	2 hrs	13 times	4 lb/ft ³ = 64 kg/m ³
FlexFoam-iT!™ V	1:1 pbv	105:100 pbw	0.08	315	50 sec.	45 min.	2 hrs	11 times	5 lb/ft ³ = 80 kg/m ³
FlexFoam-iT!™ 6	1:1 pbv	105:100 pbw	0.09	280	35 sec.	60 min.	2 hrs	10 times	6 lb/ft ³ = 96 kg/m ³
FlexFoam-iT!™ 7 FR	1:1 pbv	100:88 pbw	0.11	229	35 sec.	60 min.	2 hrs	8 times	7 lb/ft ³ = 110 kg/m ³
FlexFoam-iT!™ VIII	1:2 pbv	52.6:100 pbw	0.13	194	35 sec.	25 min.	2 hrs	7 times	8 lb/ft ³ = 128 kg/m ³
FlexFoam-iT!™ X	1:1 pbv	105:100 pbw	0.16	157	50 sec.	45 min.	2 hrs	6 times	10 lb/ft ³ = 160 kg/m ³
FlexFoam-iT!™ 14	1:2 pbv	100:190 pbw	0.22	114	60 sec.	45 min.	2 hrs	4 times	14 lb/ft ³ = 220 kg/m ³
FlexFoam-iT!™ 15	1:2 pbv	100:185 pbw	0.24	115	2 min.	90 min.	4 hrs	4 times	15 lb/ft ³ = 240 kg/m ³
FlexFoam-iT!™ 17	1:2 pbv	100:185 pbw	0.27	93	60 sec.	30 min.	2 hrs	3.5 times	17 lb/ft ³ = 270 kg/m ³
FlexFoam-iT!™ 23 FR	N/A	85:100 pbw	0.37	68	90 sec.	60 min.	2 hrs	2 times	23 lb/ft ³ = 370 kg/m ³
FlexFoam-iT!™ 25	N/A	1:2 pbw	0.40	63	90 sec.	25 min.	2 hrs	2 times	25 lb/ft ³ = 400 kg/m ³

Mixed Viscosity (ASTM D-2393): 1000 cps

Color: White

* Values measured at room temperature (73°F/23°C)

Appendix H: Equations for Gear Ratio Calculations

$$\text{Power} = \frac{\text{Work}}{\text{Time}} = \text{Force} \times \frac{\text{Distance}}{\text{Time}} = \text{Force} \times \text{Velocity}$$

$$\text{Force} = W$$

$$\text{Velocity} = v_y = v \sin$$

$$\text{Power} = W \times v \times \sin$$

$$v = \frac{\text{Power}}{W \times \sin} \quad \text{eq. x1}$$

Where W is the weight of the loaded rover and v is the velocity of the rover.

$$v = R \times \text{wheel}$$

$$\text{wheel} = \frac{v}{R} \quad \text{eq. x2}$$

Where wheel is the angular velocity of the wheels and R is the radius of the wheels.

$$N_{gb} = \text{crank} \cdot 1$$

$$1 = \frac{\text{crank}}{N_{gb}} \quad \text{eq. x3}$$

Where N_{gb} is the gear ratio of the gearbox, crank is the angular velocity of the riders' pedaling, and 1 is the angular velocity of the gearbox sprockets.

$$v_{\text{belt}} = r_1 \cdot 1 = r_2 \cdot 2$$

$$r_1 \cdot 1 = r_2 \cdot 2$$

$$r_1 \cdot n_1 = r_2 \cdot n_2$$

$$n_1 \cdot 1 = n_2 \cdot 2$$

$$N_{fd} = \frac{1}{2} \quad \text{eq. x4}$$

Where r_1 is the radius of the gearbox sprockets, r_2 is the radius of the drive shaft sprockets, n_1 is the number of teeth on the gearbox sprockets, n_2 is the number of teeth on the drive shaft sprockets, and N_{fd} is the final drive.

$$N_{fd} = \frac{n_2}{n_1}$$

$$n_2 = n_1 \cdot N_{fd} \quad \text{eq. x5}$$